EES Catalysis

REVIEW ARTICLE

View Article Online
View Journal | View Issue

Cite this: *EES Catal.*, 2025, 3, 595

Recent developments in solvent and catalyst selection for 5-hydroxymethylfurfural oxidation to 2,5-furandicarboxylic acid

Jacob M. Molinaro,[a] Joel Swartzentruber,[a] Van W. Ledger,[a] Zachary T. Fredericks,[a] David Martin Alonso[b] and Stephanie G. Wettstein *[a]

Received 31st January 2025,
Accepted 21st March 2025

DOI: 10.1039/d5ey00028a

rsc.li/eescatalysis

The sustainable and economic production of bio-monomer 2,5-furandicarboxylic acid (FDCA) remains a major hurdle on the path to widescale adoption of biomaterials like polyethylene furanoate (PEF). PEF offers several advantages over conventional petroleum-derived plastics, including enhanced material properties and reduced environmental impact, making its economic feasibility a significant topic of study in recent years. Overcoming the challenges of high catalyst costs, low product solubility, and reactant degradation are key to improving the viability of the process. In recent years, significant research has been reported using both noble and non-noble metal catalysts over a variety of supports including activated carbons, transition metal oxides, and other polymer- or ceramic-based materials. Additionally, heterogeneous catalysts have been investigated in aqueous, organic, and binary aqueous/organic solvent systems to address solubility concerns. In parallel, a better understanding of the reaction mechanism and impact of reaction conditions such as temperature, time, and additives have provided insight into the factors that influence FDCA production. In this review, we report the impact these factors have on 5-hydroxymethylfurfural (HMF) oxidation, with key focus on noble and non-noble catalysts in both aqueous and organic solutions. Additionally, we present mechanistic insights related to catalyst and solvent choice.

Broader context

This paper reviews publications that discuss 5-hydroxymethylfurfural oxidation to 2,5-furandicarboxylic acid (FDCA) over heterogeneous catalysts from the last few years. Interest in this topic has grown exponentially and this substantial review covers noble and non-noble metal catalytic systems in both aqueous and organic solvent systems. Throughout the review, trends are discussed that were found when looking at the data from multiple papers collectively, and guidelines are provided to improve the catalytic activity for FDCA production.

Introduction

Biomass is one of the most promising alternatives to replace petroleum as a source of carbon to produce chemicals. In 2004, the United States Department of Energy (DOE) identified the most promising chemical precursors that can be obtained from biomass[1] and in 2010, the list was revisited by Bozell.[2] Among these building blocks, 2,5-furandicarboxylic acid (FDCA) has become one of the most relevant, with widespread interest in increasing yields to improve the economics of the process. If economic viability is achieved, there could be further commercialization of biomass-derived plastics, an industry that holds an estimated value of several billion dollars.[1,3] Bio-based plastics have the potential to replace one of the most widely used materials for consumer goods like beverage bottles, food packaging, and textiles, polyethylene terephthalate (PET), which is derived from petroleum.[4] The process to create bioplastics starts from biomass to produce fructose, which is dehydrated to 5-hydroxymethylfurfural (HMF) then oxidized to form FDCA (Fig. 1). The final step is polymerization of FDCA to the bioplastic polyethylene furanoate (PEF). This is a similar process to petroleum plastics with prior studies indicating that it would be feasible for existing PET production lines to transition to bioplastics production with minimal changes required.[5] PEF is the primary bioplastic made from FDCA and is fully recyclable

[a] *Department of Chemical and Biological Engineering, Montana State University, Bozeman, Montana, USA. E-mail: stephanie.wettstein@montana.edu*
[b] *EQS Group (Sustainable Energy and Chemistry Group), Institute of Catalysis and Petrochemistry (CSIC), C/Marie Curie 2, 28049 Madrid, Spain*

using the same sorting technologies that are used for PET recycling.[6] Furthermore, PEF offers significant material advantages over PET including a higher glass transition temperature, improved O_2 and CO_2 barrier properties,[7] and being completely

Jacob M. Molinaro

Jacob Molinaro is a PhD candidate in Montana State University's (MSU) Chemical and Biological Engineering Department and received his BS in Chemical Engineering from Rowan University and MS in Chemical Engineering from MSU. His research focuses on upgrading biomass-derived chemicals through improved solvent and catalyst selection. This work includes experimental and computational studies of furan solubility, machine learning-based modeling of molecular interactions, and catalytic oxidation reactions to optimize furan production.

Joel Swartzentruber

Joel Swartzentruber is a graduate student in MSU's Chemical and Biological Engineering department. He received a BS in Materials Science and Engineering at The Ohio State University and has industry experience in material characterization and fabrication. Joel's research focuses on bimetallic catalyst design and production for the upgrading of biomass into renewable monomers as well as catalyst characterization.

Van W. Ledger

Van Ledger is an undergraduate Chemical Engineering student at Montana State University and has been a research assistant since June of 2024. His research focuses on solvent characterization for oxidation of 5-hydroxymethylfurfural to 2,5-furandicarboxylic acid. This includes both experimental and empirical characterization and analysis through the use of small-scale batch reactions and the design of artificial neural networks.

Zachary T. Fredericks

Zach Fredericks is an undergraduate Chemical Engineering student at Montana State University. He has been working as a research assistant since May 2024. Zach's research focuses on the effect of catalyst synthesis method on oxidation reactions. This work includes literature review, method standardization, atomic layer deposition, and characterization of catalysts via inductively coupled plasma.

David Martin Alonso

Since 2023, Dr David Martin Alonso is a Scientific Researcher at the Institute of Catalysis and Petrochemistry of CSIC (ICP-CSIC). He earned his BS in Chemical Engineering at the University of Salamanca (Spain) and his PhD at the Catalysis and Petrochemistry Research Institute (Spain), working in biodiesel production using heterogeneous catalysis. In 2009, he began working with Prof. Dumesic at the University of Wisconsin–Madison studying catalytic processes to convert biomass into chemicals and fuels. In 2012, David joined Glucan Biorenewables LLC, a start-up, as Director of Research and Development. He has over 20 years of experience in biomass conversion.

Stephanie G. Wettstein

Prof. Stephanie Wettstein is in the Chemical and Biological Engineering department at MSU. She received her BS in Paper Science at the University of Wisconsin–Stevens Point and worked as a Process Engineer in industry for three years post-graduation. Dr Wettstein then obtained her PhD from the University of Colorado in the area of zeolite membrane separations and completed a two-year post-doc at the University of Wisconsin–Madison in the area of catalysis under the guidance of Prof. Dumesic. Her research focuses on synthesizing platform chemicals, specialty chemicals, and biofuels from lignocellulosic biomass using novel catalytic and separation processes.

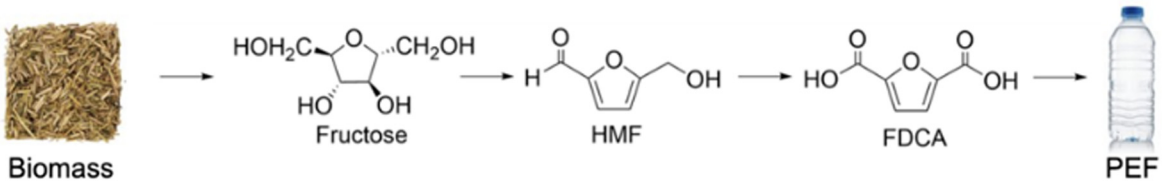

Fig. 1 Simplified scheme to produce PEF starting from biomass to produce fructose, then dehydration to HMF, oxidation to FDCA, and the final polymerization.

compostable under select conditions.[8] Although processes exist to efficiently polymerize FDCA to PEF, a bottleneck for PEF production persists in the economical production of FDCA.[9]

Increasing interest in producing FDCA can be seen in research publications throughout the last 15 years (Fig. 2), including several reviews of the subject,[10,11] with the majority of the publications focused on catalytic HMF oxidation. Today, the most effective process to oxidize HMF uses a homogeneous Mn/Co/Br catalyst and acetic acid as the solvent (AMOCO process).[12,13] A pilot-scale production plant using the AMOCO process is currently being operated in the Netherlands, but the total cost to synthesize PEF is currently estimated at twice that of PET.[14,15] Recent projections suggest that PEF will sell at $4.73–$5.92 USD per kilogram, while prices between $1.78 and $2.96 USD are necessary to be competitive.[15] Several research groups have conducted techno-economic analyses (TEAs) of FDCA production, consistently coming to similar conclusions.[3,16–18] FDCA production using the AMOCO process in its current state is not economically feasible without subsidization, and limits the sustainability and environmental benefits of the process that heterogeneous catalysts could improve. However, to drive the reaction to FDCA there is a high cost affiliated with elevated reaction temperatures and pressures[19] and in many cases, the need for additives.[17] Thus, there has been a slow adoption of FDCA for plastics manufacturing. Recent research has focused on both noble and non-noble metal catalysts using a variety of catalyst supports including activated carbons,[20–24] mixed metal oxides,[25–28] and non-oxide ceramics.[29–31] Research has also focused on a reduction in fouling[32] and sintering,[30] and an increase in catalyst recyclability,[33] to reduce economic considerations, particularly for more active noble metal catalysts.

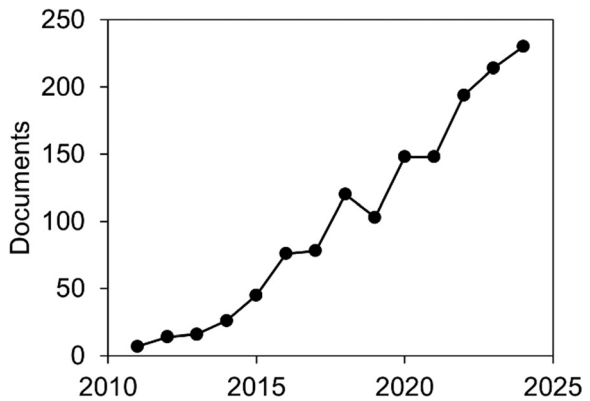

Fig. 2 Number of journal articles and reviews in the last 15 years (obtained *via* Web of Science using: 2,5-furandicarboxylic acid (Topic) AND cat* (Topic) and Article or Review Article (Document Types) and English (Languages).[31]

In addition to catalyst considerations, solvent stability and product solubility impose additional barriers to the HMF oxidation process. Solubility is of particular importance when dealing with diacids, such as FDCA, that have limited solubility in most common commercial solvents. For example, FDCA has a solubility of 0.2 wt% in water[34] and 1 wt% in ethanol[35] at STP, necessitating large solvent volumes and increased expenses with reactor sizing, material costs, and potential environmental impact. Low FDCA solubility has also been reported to result in separations and recovery challenges since FDCA can crystallize on the catalyst surface.[18,36] Though solubility can be partially mitigated by working at elevated temperatures,[36] this increases utilities costs and can lead to the degradation of sensitive furan compounds.[37] Thus, many studies have focused on reducing the expense of FDCA manufacturing by improving reaction conditions[38] and minimizing material costs using novel catalysts[7,39] and solvents.[40] While the focus of this review is on heterogeneous metal-based catalysis, other oxidative approaches have demonstrated success in HMF upgrading. Electrocatalysis, particularly using bimetallic oxides[41–43] and layered double-hydroxide catalysts,[44] has achieved high selectivity towards FDCA under mild conditions. Similarly, photocatalysis has enabled HMF oxidation using visible-light-driven materials, achieving promising results at ambient conditions.[45–47]

In 2023, a comprehensive overview of catalyst selection was published by Prasad *et al.*[48] that described the state of the field and promising directions for further catalysis research. In recent years, significant progress has been made in improving FDCA solubility and in catalyst development. This present review furthers previous work by discussing insights to the mechanism of the HMF to FDCA reaction and highlighting recent advancements in the application of heterogeneous metal catalysts to produce FDCA, with a focus on the impacts that solvent, catalyst, and catalyst support selection can have on reaction efficiency and yield.

Mechanistic insights

The oxidation of HMF to FDCA proceeds through a series of intermediates, shown broadly in Scheme 1, with the specific reaction pathway being influenced by catalyst type, solvent choice, and reaction conditions. While the process involves several oxidation steps, the overarching theme is the stepwise conversion of functional groups attached to the furan ring.

This begins with an alcohol and aldehyde group on HMF and progresses to two carboxylic acid groups on FDCA. Understanding the mechanism of this transformation provides greater insight into solvent and catalyst behaviors, potentially leading to more targeted development of reaction systems. The following section outlines the primary reaction pathways for the conversion of HMF to FDCA, discusses key intermediates, and provides insight into factors that influence selectivity.

In the initial steps of HMF oxidation, reaction conditions dictate whether the reaction proceeds through 5-hydroxymethyl-2-furancarboxylic acid (HMFCA) *via* initial oxidation of the aldehyde group or 2,5-diformylfuran (DFF) *via* initial oxidation of the alcohol group (Scheme 1). The overall oxidation process starts with HMF, a furan ring with an alcohol group attached in the 2 position and an aldehyde group attached at the 5 position. The reaction then proceeds *via* one of two intermediates, either through DFF or the less common HMFCA, depending on which functional group is oxidized first.[49] The pathway followed is affected by the catalyst, solvent, and reaction conditions chosen, which will be discussed in more detail later in the review. From either the DFF or HMFCA intermediate, additional oxidation results in the formation of 5-formyl-2-furancarboxylic acid (FFCA), which contains an aldehyde at the 2 position and a carboxylic acid at the 5 position. The final oxidation step takes place at the aldehyde of FFCA, resulting in two carboxylic acid groups in the 2 and 5 positions and the formation of FDCA.

These oxidations are facilitated by the breaking and reforming of bonds through interactions with oxidants, such as *tert*-butyl hydroperoxide (TBHP),[50,51] O_2,[21,52] or by interactions with alternate oxygen sources like water,[53,54] and over a wide variety of catalysts including both noble and non-noble metals. It is advantageous to tailor the oxidant to the specific system being studied for the minimization of side products, particularly when using organic solvents or solvent blends. However, it has been shown that oxygen pressure above 2 MPa[55] has minimal impact on the conversion of HMF to FDCA and that a homogeneous oxygen source, such as water or TBHP, is more effective.[56] In some specific cases, an excess of oxygen has been observed to lead to catalyst poisoning,[57] suggesting that moderate pressures and concentrations may be optimal for HMF oxidation.

Initial 5-hydroxymethylfurfural reaction

For the first, more common pathway, the alcohol group of HMF is oxidized to an aldehyde, forming DFF (Scheme 2), which according to Chen, G. *et al.*,[54] had a 29% lower activation energy than forming HMFCA using a Co–Mn–Br catalyst. This may be due to steric hindrance on the bulkier aldehyde group, making it more energetically favorable for the alcohol to coordinate with a catalyst. This alcohol coordination can also be facilitated through the presence of Lewis acid–base chemistries. Lewis-base sites on the metal catalyst surface interact with the mildly acidic hydroxyl hydrogen and weaken the carbinol C–H bonds, preparing the site for attack by a hydroxy radical. This radical can be sourced from either a peroxide, such as TBHP or hydrogen peroxide (H_2O_2), from water, or a homogeneous base such as sodium hydroxide (NaOH).[58] The hydroxy radical reacts with a scavenged hydrogen from HMF and forms water, while the carbinol carbon is left with an unbonded electron pair (Scheme 2, top). This remaining lone pair facilitates the formation of a pi-bond with the oxygen in the alcohol, weakening the O–H bond and allowing for an oxidant radical, such as ($^{\bullet}$OH), to accept the hydrogen, resulting in a side product and the formation of DFF (Scheme 2, bottom). For example, using TBHP as an oxidant and *tert*-butyl alcohol (TBA) as a solvent,[50] TBHP decomposes to form two radicals: *tert*-butoxy (*t*-BuO$^{\bullet}$) and hydroxy ($^{\bullet}$OH). The hydroxy oxidizes the –OH group of HMF, forming DFF, while the *tert*-butoxy radical reforms as TBA *via* the addition of hydrogen ions.

An alternative reaction pathway to FDCA is to first oxidize the aldehyde group on the HMF molecule (Scheme 1). Some selectivity to HMFCA is observed even under reaction conditions that favor the DFF pathway; however, researchers have reported that the addition of peroxide[59] or use of specific catalysts can increase selectivity towards the HMFCA pathway.[60,61] It has been found that silver (Ag) catalysts are of particular use for selectivity towards HMFCA, with the most common choice being in the form of AgO_2 or $AgNO_3$.[60,62] In aqueous media, the alkaline nature of the Ag(I) catalyst can prime the acidic carbonyl carbon of the aldehyde for conversion towards the diol intermediate (Scheme 3), as has also been reported in other aldehyde oxidation reactions.[60,63] Additionally, other novel catalysts have recently been found that are selective to

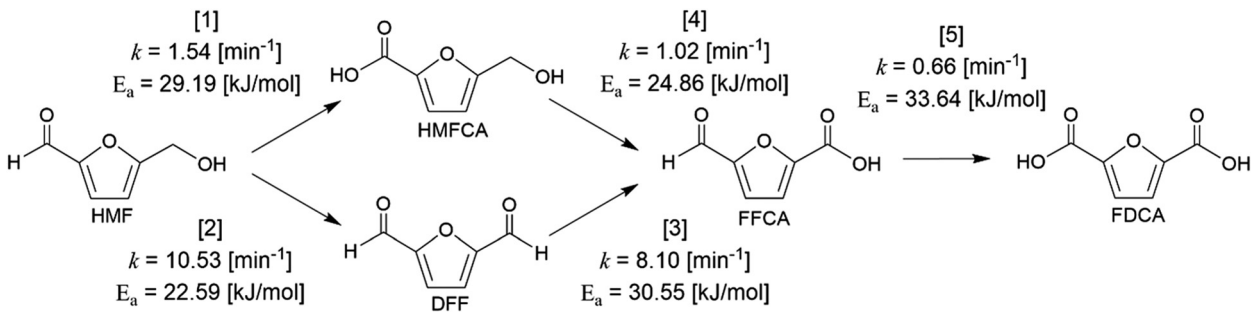

Scheme 1 HMF to FDCA reaction pathway with kinetic parameters from a semi-batch reaction using an acetic acid solvent and Co/Mn/Br catalyst at 413 K (adapted from Chen *et al.*[49]).

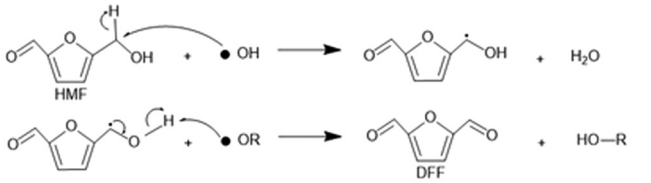

Scheme 2 Reaction mechanism for the oxidation of HMF to DFF. A hydroxy radical attacks the carbinol carbon of the alcohol before a secondary oxidant facilitates the formation of a π-bond.

HMFCA including those incorporating Mn in the 4+ valence state[59] and Mo in the 6+ valence state.[64]

The geminal diol intermediate, though unstable and not observed as a side product, is critical for converting the aldehyde to a carboxylic acid (Scheme 3). Following its formation, the geminal diol acts as a Brønsted–Lowry acid and gives up a hydrogen ion from its β-carbon. This elimination forms water or another side product and allows for the formation of a π-bond between the β-carbon and one of the alcohol groups. This alcohol group releases a hydrogen ion as well, completing the transition to HMFCA. As observed for the formation of DFF, a range of different oxidants can be used for the conversion to HMFCA, though the most common include water and peroxides like H_2O_2.[59,62]

Intermediates to 2,5-furandicarboxylic acid

The reaction mechanisms from DFF or HMFCA to FFCA and FDCA follow similar chemistries to those presented for the conversion of HMF to DFF (an alcohol oxidation) and HMF to HMFCA (an aldehyde oxidation). DFF has two aldehyde groups, one at the 2 position and one at the 5 position, and both of these aldehydes must be converted to carboxylic acids for the formation of FDCA (Scheme 4). For HMFCA, both the alcohol and the carboxylic acid groups undergo oxidation (Scheme 5). For DFF, the first oxidation targets one of the aldehydes and proceeds through the previously presented geminal diol intermediate (Scheme 4). The second oxidation targets the unconverted aldehyde group, ultimately forming FDCA (Scheme 6). The alcohol group first oxidizes to an aldehyde *via* the hydroxy radical attack and π-bond formation, producing FFCA (Scheme 5).

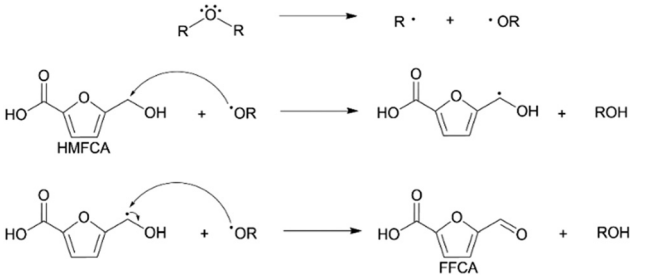

Scheme 5 Reaction mechanism for the oxidation of HMFCA to FFCA. A hydroxy radical attack first targets the carbinol carbon of the alcohol group before a second oxidant results in the formation of a π-bond.

It then undergoes further oxidation *via* the geminal diol intermediate and β-elimination to form FDCA (Scheme 6).

As reported by the mechanistic and kinetic studies of Chen *et al.*,[49] the activation energies required to proceed along the reaction pathway increase with each subsequent oxidation step, likely increasing with molecular bulkiness and increasing steric hindrance. (Scheme 1) Following this trend, the limiting step of the overall HMF to FDCA process is the final aldehyde oxidation of FFCA to FDCA.[49] Starting with HMF and progressing through either DFF or HMFCA to FFCA and ultimately FDCA, the oxidation process presents opportunities for intricate reaction engineering through alteration of solvents, catalysts, and reaction conditions.

Aqueous reactions

Water, with or without the addition of a base (such as NaOH) is the most reported solvent for the oxidation of HMF to FDCA due to its low cost, availability, and in the case of bases, increased solubility of FDCA.[10,48] Water has been shown to be an effective solvent for HMF oxidation, often achieving FDCA yields exceeding 80% across a range of reaction conditions. This is largely due to water's donation of hydroxy radicals and its low interactivity with the functional groups present in furan compounds (Scheme 1).[52]

Despite high HMF conversion and FDCA yields, purely water-based reactions are typically run at low HMF concentrations

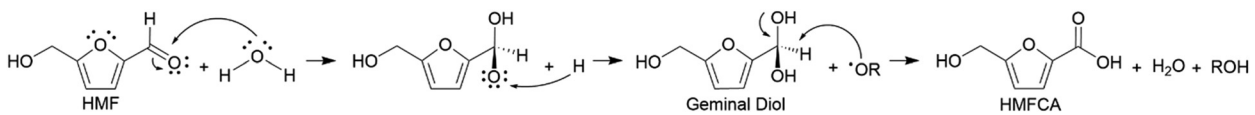

Scheme 3 Reaction mechanism for the oxidation of HMF to HMFCA. The conversion of the aldehyde to a carboxylic acid is facilitated through a geminal diol intermediate followed by a β-hydride elimination.

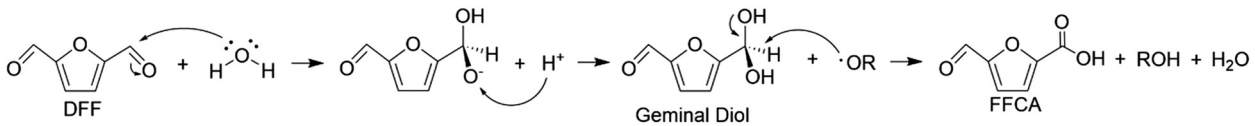

Scheme 4 Reaction mechanism for the oxidation of DFF to FFCA. The conversion of an aldehyde to a carboxylic acid progresses through the geminal diol intermediate before a β-hydride elimination allows the formation of a new C═O bond.

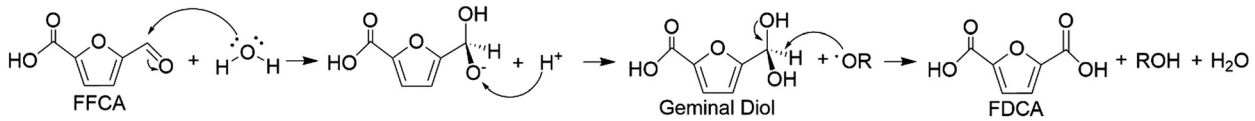

Scheme 6 Reaction mechanism for the oxidation of FFCA to FDCA. The remaining aldehyde of FFCA is converted to a carboxylic acid *via* a geminal diol intermediate and a β-hydride elimination.

(<1.25 wt% HMF) due to the low solubility of FDCA which can precipitate on the catalyst surface and deactivate the catalyst.[58,65,66] Adding bases to form the corresponding FDCA salt increases solubility across a range of additives including $KHCO_3$,[67] $NaHCO_3$,[68] Na_2CO_3,[30] and, most commonly, NaOH,[69,70] which helps avoid catalyst deactivation resulting in higher FDCA yields when operating at HMF concentrations greater than 2 wt%. However, the use of an excess of base should be carefully considered. It has been shown that a 0.3 M NaOH solution converted 10% HMF even without catalyst present (t = 0.5 h; T = 295 K),[71] and an overly caustic of a reaction solution can cause HMF degradation to formic acid and 2,5-bis(hydroxymethyl)furan (BHMF).[71] Vuyyuru and Strasser reported that during a 10 h observation period at 333 K, nearly 80% of HMF degraded in the presence of NaOH (pH 13).[70] Caustic reaction solvents also lead to increased safety hazards, reactor vessel and piping material considerations, and additional processing steps to neutralize solvents before discharge. While increased base content and the subsequent presence of hydroxide ions improves FDCA solubility and catalytic activity, carbon loss due to furan degradation must be considered.

A growing movement towards base-free oxidation focuses on using specially engineered catalysts or non-caustic additives to improve reaction efficiency.[58,72–74] For example, with the addition of metal or oxide catalysts, higher HMF conversions and FDCA yields have been shown possible at comparable temperatures and at higher initial HMF concentrations (>2 wt% HMF) in batch reactors.[20,25,50,75] In the following sections, the impact of additives, catalyst type, and reaction conditions will be discussed to determine key trends for improving HMF conversion and FDCA yields in aqueous solvent systems.

Noble metal catalysts

Noble metal catalysts, such as platinum (Pt), palladium (Pd), gold (Au), silver (Ag), and ruthenium (Ru), are commonly used in industrial processes for the upgrading of organic molecules.[76,77] This is true for HMF oxidation as well, with many publications prior to 2020 focusing on the use of noble metals as catalysts, which offer advantages such as overcoming high reaction activation energy and exhibiting better reusability, while non-noble metal catalysts are desirable for their lower cost and lesser environmental impact. Noble metals also have significant advantages such as improved catalytic activity, anticorrosion properties, and stability. These properties are corollary behaviors to the highly stable structures of noble metals, which have fully or mostly filled d-electron orbitals and only two or three possible oxidation states (Table 1).[10] The exception to this statement is Ru, which has been frequently applied in HMF catalysis in unique ways compared to other noble metals.

Table 1 Oxidation states and electron orbital configurations of different noble metals

Metal	Possible oxidation states	Electron orbital configuration
Pt	0, +2, +4	[Xe] $4f^{14}$ $5d^9$ $6s^1$
Pd	0, +2, +4	[Kr] $4d^{10}$
Au	0, +1, +3	[Xe] $4f^{14}$ $5d^{10}$ $6s^1$
Ag	0, +1	[Kr] $4d^{10}$ $5s^1$
Ru	0, +2, +3, +4, +6, +8	[Kr] $4d^7$ $5s^1$

These metals can be supported on a range of materials including activated carbon (AC), transition metal oxides, or non-oxide ceramics. Such materials often enhance the catalytic activity of the metals on the support by increasing electron transfer, particle distribution, or increasing the available surface area for reactant adsorption.

Platinum

Platinum catalysts typically provide high HMF conversion, high FDCA yields, and are resistant to fouling, allowing hydroxide ions to adsorb and interact with reactants more efficiently.[78] They have been effectively applied to the oxidation of HMF for a range of solvents and reaction conditions and often serve as a baseline for novel catalyst development. In regards to HMF oxidation, Pt catalysts have been used at a range of temperatures and have been shown to be active on various supports.

On a carbon support with no base addition, a recent study by Ryu *et al.* observed that higher catalyst to HMF ratios for shorter reaction times (Table 2, index 1) resulted in 10% more FDCA compared to longer reactions at lower catalyst loadings (Table 2, index 2), with yields ranging from 80–90%.[52] In another study, Yang *et al.* prepared platinum catalysts supported by nitrogen-doped carbon (NC), then stabilized the Pt nanoparticles (NPs) using polyvinyl alcohol (PVA). The NC supports were made from pomelo peel and attained different surface areas based on the carbonization temperature (673, 873, or 1073 K). The reactions used $NaHCO_3$ as a base additive. The supports studied, NC-400 (Table 2, index 3), NC-600 (index 4), and NC-800 (index 5), had S_{BET} values of 513, 740, and 809 m^2 g^{-1}, respectively, with both pore volume and average pore diameter increasing in parallel to overall surface area. Compared to both a traditional, commercially available AC support (Table 2, index 6) and the lower S_{BET} prepared supports (indices 3 and 4), the NC-800 support (index 5) that was synthesized with the highest carbonization temperature, reported the highest FDCA yields of 83.9% at 100% HMF conversion and lower percentages of intermediates.[79]

Table 2 Platinum catalysts that have been studied for aqueous-based HMF oxidation

Index	Catalyst	Support	Base	t (h)	T (K)	P_{O_2} (MPa)	$C_{HMF,i}$ (wt%)	HMF/Cat. (mol mol^{-1})	HMF Conv. (%)	FDCA yield (%)	Ref.
1	Pt	Carbon	—	2.5	393	1	1.00	50	100	89.7	52
2	Pt	Carbon	—	3	393	1	3.00	75	100	80	52
3	Pt	NC-400	$NaHCO_3$	24	383	0.5	0.63	200	98.8	1.3	79
4	Pt	NC-600	$NaHCO_3$	24	383	0.5	0.63	200	99.9	2.5	79
5	Pt	NC-800	$NaHCO_3$	24	383	0.5	0.63	200	100	83.9	79
6	Pt	Carbon	$NaHCO_3$	24	383	0.5	0.63	200	100	66.8	79
7	Pt	UiO-66	—	14	408	0.5	0.31	200	99	68	74
8	Pt	MIL-101 (Cr)	—	14	408	0.5	0.31	200	98	28	74
9	Pt	Boehmite	—	14	408	0.5	0.31	200	98	19	74
10	Pt	PVP-UiO-66	—	14	408	0.5	0.31	200	99	46	74

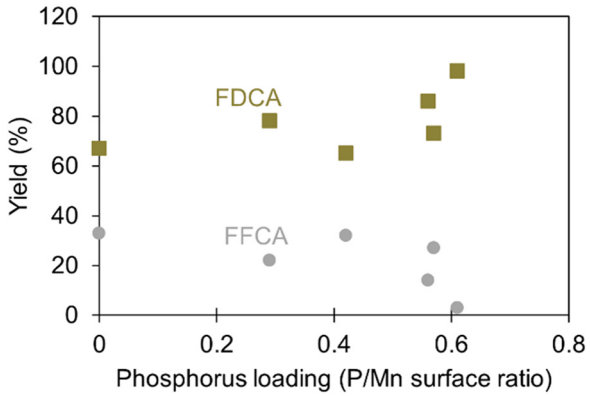

Fig. 3 Impact of P dopant amount on the surface of the catalyst (determined by XPS) on FDCA (■) and FFCA (■) yields for MnP_yO_x catalyst (100% HMF conversion for all). Reaction conditions: 100 : 1 HMF : Pt molar ratio, 1.25 wt% HMF, T = 383 K, P_{O_2} = 1 MPa, 24 h.[58]

A base-free study by Hou *et al.*[58] found that although the surface area of the catalyst did trend with FDCA yield, in most cases, the amount of phosphorus (P) on the support also contributed to the activity of the catalyst (Fig. 3). Maintaining standard reaction conditions, levels of P doping on a manganese (Mn) oxide support were varied and compared to non-doped MnO_2, which converted 100% of the HMF with 67% FDCA selectivity. Increased ratios of P/Mn on the catalyst surface peaked at the highest P/Mn surface ratio evaluated and resulted in 98% FDCA selectivity at 100% HMF conversion (Fig. 3). However, this catalyst did not have the highest P/Mn bulk ratio (determined by ICP-MS). Increasing the P/Mn ratio from the optimal 0.50 to 0.55 and 0.59 decreased the FDCA yield to 73% (0.57 P per Mn surface ratio) and 66% (0.42 P per Mn surface ratio), respectively, while increasing the FFCA yield.

The decreased activity of the catalyst at increased P concentrations may be due to the lower P amount at the surface or the formation of stronger Mn–P–O interactions that decrease the availability of oxygen for use as an oxidizing agent. The presence of phosphorus in the support was noted to help maintain the metallic (Pt^0) state of Pt and facilitate the reduction of MnO_x to stabilize at Mn^{4+} and Mn^{3+} states.[58] This aligns well with prior discussion of P-doping and its impact on catalytic activity elsewhere in the literature.[80]

The importance of maintaining Pt in its metallic (Pt^0) state was also reported by Seehamongkol *et al.*,[74] who investigated the catalytic activity of Pt nanoparticles (NPs) on metal–organic frameworks (MOFs). At 98–99% HMF conversion, Pt without surfactant on a zirconium oxide MOF (UiO-66) support resulted in the highest FDCA yields of near 70% (T = 408 K, P_{O_2} = 0.5 MPa; Table 2, index 7). Comparatively, a MIL-101 (Cr) MOF reported a 28% yield (index 8), Boehmite reported a 19% yield (index 9), and polyvinylpyrrolidone (PVP)-stabilized Pt on UiO-66 reported a 46% yield (index 10). Both catalysts with and without PVP-stabilization produced 2% FFCA as a side product whereas the Boehmite and MIL-101 (Cr) supported catalysts resulted in 7% and 20% FFCA, respectively.[74] Much like the supports studied by Hou *et al.*, the UiO-66 MOF was proposed to offer the greatest availability of basic sites and adsorbed oxygen species. Also, in the case of Pt/UiO-66, the relative oxidation state distribution of Pt^0 was higher compared to Pt-PVP/UiO-66 and Pt/MIL-101(Cr) resulting in higher FDCA production. Additionally, the researchers hypothesized that the PVP-stabilized catalyst had lower activity due to the limited substrate accessibility as a result of polymers blocking active sites,[74] which has also been seen in prior literature.[30,81]

Temperature is another relevant factor in FDCA selectivity, as reported in multiple places in the literature, as kinetic studies on the decomposition of HMF have shown that the decomposition rate constant doubles with every 25 K of increasing temperature.[82] When the $Pt/MnP_{0.50}O_x$ catalyst was tested across a range of temperatures, an expected increase in FDCA yield occurred (Fig. 4; filled squares).[58] A similar increase in FDCA yield from 11% (368 K) to 68% (408 K) was observed when using the previously discussed Pt/UiO-66 catalyst; however, at 423 K, the FDCA yield decreased to 62% (Fig. 4; open squares).[74] This decrease in yield was hypothesized to be due to HMF degradation at the higher temperature,[74] which has been shown in other studies as well. HMF degradation has been reported to typically begin around 403 K with some variability due to reaction conditions like solvent selection or the presence of additives, decreasing selectivity. Similar observations have been reported in the literature, with downturns in FDCA production at 423 K in methanol[23] and above 393 K in ACN.[27]

Among the most significant factors impacting catalyst activity were overall surface area, the addition of stabilizers such as PVA or PVP, and reaction temperature. Polymeric stabilizers run the risk of reduced yields, as they can block active sites and reduce effective catalyst surface area. Higher surface areas for a given catalyst type correlated with higher FDCA yields due to an

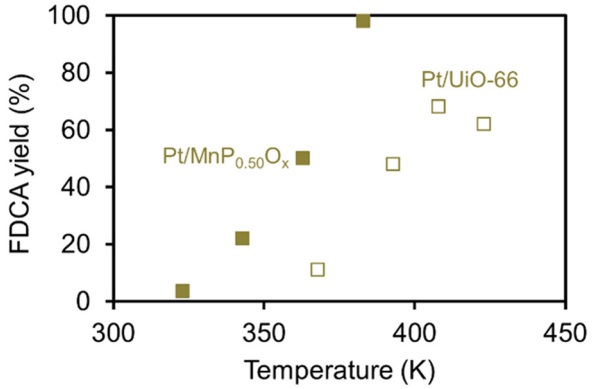

Fig. 4 Effect of reaction temperature on FDCA yield with a Pt/UiO-66 catalyst (□)[74] and a $Pt/MnP_{0.50}O_x$ catalyst (■).[58] Reaction conditions for Pt/UiO-66 catalyst: HMF : Pt 200 : 1 molar ratio, P_{O_2} = 0.5 MPa, t = 14 h[74] and for $Pt/MnP_{0.50}O_x$ catalyst: HMF : Pt 100 : 1 molar ratio, P_{O_2} = 1 MPa, t = 24 h.[58]

increased number of active sites and capacity for reactant adsorption on the surface of the catalyst. Additionally, the availability of Lewis-base sites and surface-adsorbed oxygen species to promote the oxidation of furan compounds must be considered. Pt was most effective in its metallic state (Pt^0), likely because it was most capable of accepting or donating a d-orbital electron. Increasing temperature and time improved HMF conversion and yield, but with diminishing returns as temperatures above approximately 408 K resulted in lower FDCA yields, likely due to HMF degradation.

Gold and palladium

In recent years, Au has been commonly reported for the catalytic oxidation of HMF,[30,65] often as a bimetallic catalyst with Pd,[20,83] Ag,[68] Ni, Fe, and Cu[73] as secondary metals. The additional metal stabilizes Au NPs, as pure Au tends to leach from supports or sinter into larger particles at elevated temperatures.[30] Larger particles tend to be less evenly dispersed, have lower surface area to volume ratios, and have fewer active sites compared to an equivalent weighting of smaller, more evenly distributed particles.

Kharlamova *et al.*[83] evaluated multiple synthesis techniques that resulted in different average particle sizes of Au, Pd, and bimetallic AuPd over a ZrO_2 support (Table 3). They found that for pure Au, decreasing particle size correlated with increasing FDCA yields. Deposition–precipitation had the smallest grain size (9 nm) and highest yield (13.4%), followed by impregnation–reduction under basic conditions (15 nm; 12.3%), impregnation–reduction under acidic conditions (30 nm; 5.0%), and incipient wetness impregnation (70 nm; 5.9%). Somsri *et al.* similarly noted higher yields with smaller particle sizes when comparing Au catalysts on CaZSM-5 supports synthesized *via* two different methods, incipient wetness (IW; Table 4, index 1) and deposition–precipitation (DP; Table 4, index 2). The catalysts produced using an incipient-wetness method resulted in a smaller average size of Au particles and led to significantly higher FDCA yields compared to catalysts synthesized with a deposition–precipitation method (Table 3).[30] The contrast in particle size relative to preparation method in the two studies indicates that there are additional factors influencing the effectiveness of the preparation method but highlights the importance of smaller Au particles for increasing FDCA yields.

The same correlation between particle size and FDCA yield was not seen with Pd (Table 3), where larger particle sizes resulted in the highest FDCA yields. In most Pd reactions, the conversion of HMF was low and for both the single metal Au and Pd reactions the majority of HMF converted to HMFCA and FFCA (Fig. 5).[83] The alkaline conditions were more effective for the pure Au catalyst while the acidic chemical reduction technique resulted in higher FDCA yields for both the pure Pd and the bimetallic AuPd catalyst. For the bimetallic AuPd catalysts, the synthesis method had a much larger impact, where incipient wetness and deposition–precipitation methods resulted in low FDCA yields, but impregnation–reduction methods resulted in higher conversions and yields (Table 3). For basic conditions, the FDCA yield was 37.3% and for acidic conditions, impregnation–reduction synthesis resulted in FDCA yields of 77.9%. The researchers attributed this higher activity to the presence of $Au_{1-x}Pd_x$ nanoparticles that cause a synergistic effect due to the electron redistribution of the metals, which favors initial HMF oxidation through the hydroxyl group (Scheme 2) *versus* the HMFCA intermediate.[83]

When comparing the Au/Pd catalysts produced by impregnation–reduction under acidic conditions on ZrO_2 supports to those produced by depositing Au on a commercial Pd/C catalyst using a deposition–precipitation method, both achieved high HMF conversion, but the product distributions differ (Fig. 5). On the ZrO_2 support, single metal catalysts of Au and Pd showed

Table 3 Effects of different catalyst synthesis techniques for aqueous HMF oxidation using ZrO_2 supports[68] and CaZSM-5 supports (marked with *).[24] For synthesis methods: IW = incipient wetness impregnation; DP = deposition–precipitation; IRB = impregnation–reduction under basic conditions; IRA = impregnation–reduction under acidic conditions

	Au				Pd				AuPd			
Synthesis method	Wt%	Particle size (nm)	HMF Conv. (%)	FDCA yield (%)	Wt%	Particle size (nm)	HMF Conv. (%)	FDCA yield (%)	Wt%	Particle size (nm)	HMF Conv. (%)	FDCA yield (%)
IW	2.1	70	74.5	5.9	2.0	2.3	6.5	0.1	1.2/0.9	NR	10.5	0.6
IW*	0.8	3.6	100	75.1	—	—	—	—	—	—	—	—
DP	1.2	9	100	13.4	2.5	2.2	15.5	0.8	0.4/0.9	NR	26.3	1.3
DP*	0.84	1.3	99.8	20.6	—	—	—	—	—	—	—	—
IRB	1.2	15	93.6	12.3	1.6	5.2	72.5	6.4	1.3/0.9	NR	95.2	37.3
IRA	2.0	30	91	5	1.6	25	76.9	6.5	1.4/0.7	24	100	77.9

Table 4 Gold and palladium catalysts studied for aqueous HMF oxidation

Index	Catalyst	Support	Base	t (h)	T (K)	P_{O_2} (MPa)	$C_{HMF,i}$ (wt%)	HMF/Cat. (mol mol^{-1})	HMF Conv. (%)	FDCA yield (%)	Ref.
1	Au–Pd(imp)	ZrO_2	$NaHCO_3$	24	353	0.5	0.63	100	13.8	0.5	83
2	Pd–Au(imp)	ZrO_2	$NaHCO_3$	24	353	0.5	0.63	100	59.1	4.6	83
3	$Au_{1.5}Pd$	C	NaOH	6	333	0.3	5.93	110	99	70	20
4	$Au_{1.5}Pd$	C	$NaHCO_3$	6	363	0.3	5.93	110	96	27	20
5	Au	MnO_2	—	12	373	0.1	0.99	20.9	75.7	52	65
6	Au	MnO_2	—	12	373	0.1	0.99	9.3	99	93.2	65

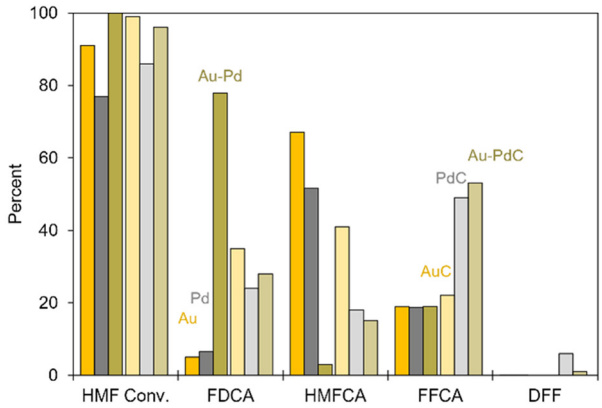

Fig. 5 Product yields for reactions using impregnation–reduction under acidic conditions synthesized catalysts using Au (■), Pd (■), and Au–Pd (■) on ZrO_2[83] and deposition–precipitation method on Au/C (■), Pd/C (■), and Au–Pd/C (■) catalysts.[20] Reaction conditions for impregnation–reduction catalyst: 100 : 1 HMF : catalyst molar ratio, 0.2 mol $NaHCO_3$, 0.63 wt% HMF, T = 353 K, P_{O_2} = 0.5 MPa, and t = 24 h.[83] For deposition–precipitation catalyst: 110 : 0.93 : 0.07 HMF : Pd : Au molar ratio, 20 mmol $NaHCO_3$, 5 mmol HMF, T = 363 K, P_{O_2} = 0.3 MPa, and t = 6 h.[20]

low FDCA yields, favoring HMFCA and FFCA under the reaction conditions. In contrast, the bimetallic Au–Pd/ZrO_2 catalyst exhibited high selectivity to FDCA.[83] On carbon supports, both single metal and bimetallic Au and Pd catalysts produced FDCA yields ranging from 24–35%. Pure Au produced more HMFCA (41% yield) while both Pd and Au/Pd catalysts generated more FFCA (49% and 53% yields, respectively) after 6 h. Extending the reaction time for the Pd/C catalyst to 9 h increased both HMF conversion and FDCA yield by approximately 4% while the FFCA, HMFCA, and DFF yields all decreased slightly.[20] Kharlamova *et al.* ran reactions for 24 h and achieved higher FDCA yields, comparatively. However, when the Au–Pd/ZrO_2 catalyst was run at shorter times (4 h), the HMF conversion (~78%) and FDCA yield (~5%) were lower while yields of intermediate products increased: HMFCA (~18%) and FFCA (~55%).[83] This indicates that the intermediates may have been converted to FDCA if the reaction was run for a longer time over the carbon supported catalysts.

Another option to improve the reaction is to add base. When a strong base, NaOH, was used, the HMF conversion increased to nearly 100% for both single metal Au and Pd catalysts at all ranges of the Au–Pd catalysts. Additionally, the FDCA yields increased to approximately 70% for the bimetallic Au–Pd catalysts with single digit percents of HMFCA forming and no detectable DFF or FFCA present (Table 4; index 3). This was attributed to the presence of hydroxide ions from the strong base, which resulted in the formation of a geminal diol intermediate and a preference for the HMFCA pathway as shown in Scheme 3.[20] Peng *et al.* also evaluated different Au loadings onto the 10% Pd/C catalyst, ranging the percent of Au from 0.75 to 4.5 wt%. Changing the Au loading had a limited effect on the HMF conversion (92–97%) or the FDCA yield (23–31%) when NaOH (Table 4, index 3) or $NaHCO_3$ (Table 4, index 4) bases were added. However, when they evaluated the rate of reaction with $NaHCO_3$ as the base, the reaction rate increased as the amount of Au on the catalyst increased.[20] Zeng *et al.* also studied the effect of metal loading by investigating Au catalysts on an MnO_2 support at loadings of 2.5 and 5.6 wt% Au. Increasing the loading of Au from 2.5 wt% (Table 4, index 5) to 5.6 wt% (Table 4, index 6) increased HMF conversion from 75.7% to 99%, and FDCA yields from 70.2% to 97.7%.[65] As the number of active sites available increased with Au loading, the catalytic performance also increased. They also attributed improved catalytic activity to the higher ratio of Au : Mn as metal–metal interactions were reported to form superoxide ions (O_2^-), leading to enhanced oxidation.[65]

Su *et al.* also used a metal oxide support, $MgAlO_x$, which held Au particles in a negative state and improved oxidation.[73] Additionally, they created Au-based bimetallic catalysts that contained approximately 1.1 wt% Au and 0.018 to 0.031 wt% of the additive metal, finding that the metal altered product selectivity and changed the electron density of Au species. Across all bimetallic Au–M catalysts studied, FDCA yields were observed to increase, except for Au–Cu. The Au–Ni catalyst achieved the highest conversion (100%) and yield (76.6%) amongst the studied bimetallic catalysts (Fig. 6).[73] Fe and Ni were both observed to promote HMF and HMFCA oxidation, while Pd was more effective at the promotion of FFCA oxidation. Pd has been previously cited as enhancing the stability of Au catalysts through improved electron transfer and modulation of electron structure in bimetallic catalysts,[84] making it a commonly used additive metal to Au. The lower activity of the Au–Cu catalyst may be attributed to the similar electron structures of the two metals, which are both group 11 elements with one valence electron. Differing valence structures, such as those observed in the Au–Ni catalyst (with 1 and 2 valence electrons, respectively), may lead to greater electron density and thus catalyst activity. Furthermore, the improved FDCA yields over Au–Ni compared to Au–Pd may also relate to the atomic structures of the dopant metal. Ni, a smaller atom, has three fewer electron shells than Pd, making it more reactive even though they are both group 10 metals. This higher reactivity may correlate to better reactant adsorption compared to the

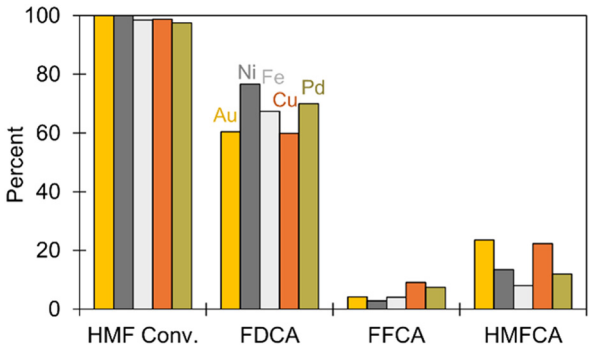

Fig. 6 Yields and conversion of adding metals to an Au/$MgAlO_x$ catalyst Reaction conditions: 70 : 1 HMF : metal molar ratio, 0.25 wt% initial HMF, T = 363 K, P_{O_2} = 0.5 MPa, and t = 2 h.[73]

more stable Pd, allowing the Au portion of the catalyst to more effectively oxidize towards FDCA.

Using a SiO_2 support, de Boed *et al.*[68] synthesized bimetallic catalysts using various amounts of Au and Ag but maintained an HMF : catalyst molar ratio of 72 : 1. They found that with a pure Au catalyst the HMF conversion was 100% and that approximately 40% FDCA and 60% HMFCA were produced. When Ag was added up to 0.18 mass fraction, the HMF conversion remained at 100%, but the FDCA yields increased to over 90% while the HMFCA dropped proportionately (Fig. 7a). Increasing the mass fraction of Ag to over 0.2 decreased the HMF conversion and FDCA yield, again favoring HMFCA production. Using only Ag on SiO_2, there was no FDCA or HMFCA produced even though the HMF conversion was 81%.[68] Ke *et al.*[60] also found that using a pure Ag catalyst resulted in no FDCA production. Continuing to add up to 0.4 mg of Pt to the initial 0.1 mg of $AgNO_3$, decreasing the mass fraction of silver to 0.2 still did not produce FDCA (Fig. 7b). Below the Ag mass fraction of 0.2, as the Pt loading and the overall ratio of catalyst to reactant increased, both conversion of HMF and selectivity to FDCA increased. The initial metal ratio of 2.8 : 1 Pt : Ag (143 : 1 HMF : catalyst) resulted in 26% HMF conversion, primarily to HMFCA. However, increasing the Pt loading further while keeping the $AgNO_3$ at 0.1 mg (12 : 1 HMF : catalyst), increased FDCA yields up to approximately 86% FDCA at 100% HMF conversion.[60] As previously observed during discussion of mechanistic insights, Ag^{1+} negatively impacted FDCA selectivity by targeting HMFCA production instead.

As noted in the Pt section, temperature can also affect the reaction. Zeng *et al.*[65] studied temperature effects over a range of 333 K to 373 K using the previously mentioned 5.6 wt% Au/MnO_2 catalyst. As the temperature increased, the HMF conversion stayed relatively constant around 90% until 373 K, at which point it was almost 100% (Fig. 8). However, the product selectivity varied across the temperature range. At low temperatures, HMFCA was present in significant amounts, with lower yields of FDCA and little FFCA, but as the temperature increased, higher amounts of FDCA and FFCA were produced, reaching 94.1% FDCA selectivity at 373 K,[65] which indicates

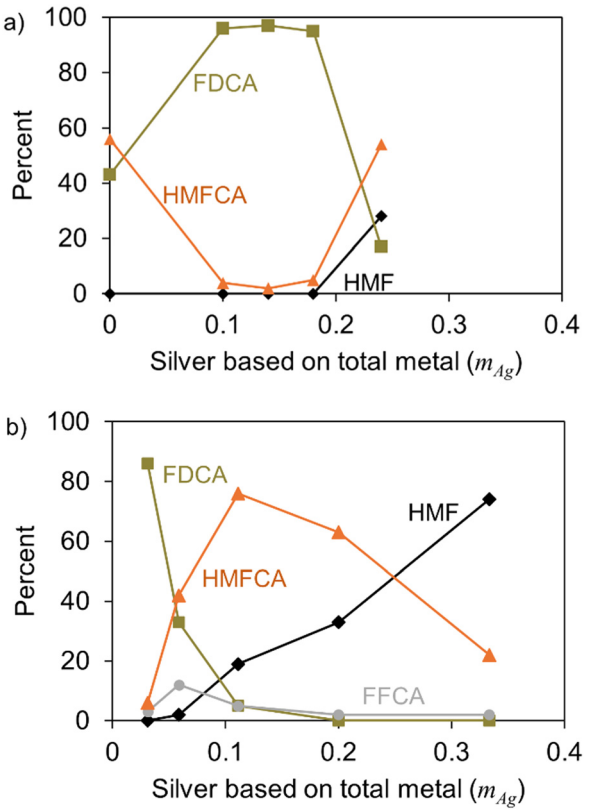

Fig. 7 Effect of silver loading on a bimetallic (a) Au/Ag SiO_2 catalyst (conditions: 79 : 1 HMF : Au molar ratio, 0.4 mmol $NaHCO_3$, T = 353 K, P_{O_2} = 1 MPa, and t = 6 h)[68] and (b) Pt/Ag catalyst where the x-axis represents the mass fraction of Ag of the total mass of the metals. Reaction conditions: 50 : 1 HMF : Pt molar ratio, 0.8 mmol $NaHCO_3$, T = 373 K, O_2 bubbling at 75 mL min^{-1}, and t = 1 h.[60]

that the higher temperatures were critical for proceeding along the reaction pathway.

In summary, Au is an effective single metal catalyst but can suffer from stability issues at elevated temperatures. At these higher temperatures, Au may leach from the support surface or sinter, leading to a reduction in catalyst surface area and thus, a lower number of active sites to facilitate furan conversion. Particularly when stabilized by other metals or organic compounds, the stronger that Au NPs interact with the support, the less likely sintering and catalyst deactivation is to be observed.[85] The addition of other metals, particularly elements that are not a part of the same group on the periodic table, to create bimetallic catalysts can improve yields. From the example of Su *et al.*,[73] Cu and Au both have one valence electron and did not perform as well as Ni/Au catalysts, which had different numbers of valence electrons. The addition of bases over Au catalysts reported significant HMF degradation, though they typically also bolstered FDCA selectivity. As was observed with Pt, many different types of support could be used to achieve high FDCA yields.

Ruthenium

Aside from Au, Ru is the most common metal studied for application in HMF oxidation in recent years. Ru is unique

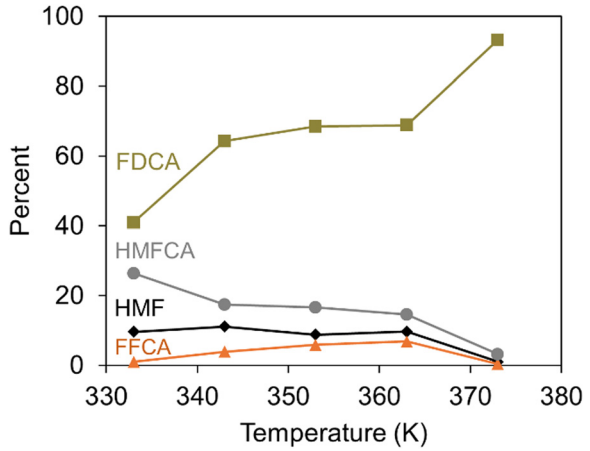

Fig. 8 Remaining HMF (♦) and product yields of FDCA (■), HMFCA (●), and FFCA (▲) for a 5.6 wt% Au catalyst on MnO_2. Reaction conditions: 9.3 : 1 HMF : catalyst molar ratio, and t = 12 h.[65]

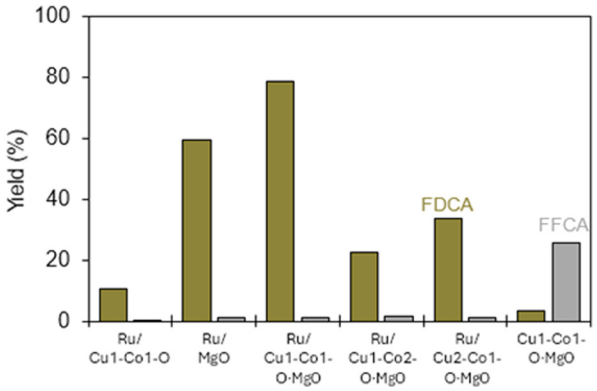

Fig. 9 Support and metal effects on FDCA (■) and FFCA (■) yields for HMF oxidation using 4 wt% Ru (when noted) on various Cu, Co, and Mg oxides supports. Reaction conditions: 0.5 wt% HMF, T = 383 K, P_{O_2} = 1 MPa, t = 12 h.[66]

among noble metals due to its vast range of potential oxidation states (Table 1), high stability, and relatively low cost compared to other noble metals. It also tends to be more resistant to some of the issues that impact other noble metals, including sintering, leaching, and oxidation. Across several studies that recycled Ru-based catalysts, FDCA yields were found to decrease by less than 5% when used for 4–6 cycles.[66,75,86] Such recyclability was attributed in one case to polymeric stabilizing agents,[86] but more commonly to the interactions between Ru and the support that helped stabilize Ru NPs.[87] These catalytic properties make Ru an attractive metal for HMF oxidation.

Many different supports have been used with Ru catalysts to achieve high yields (Table 5). Zheng *et al.*[87] investigated a range of metal oxide supports, comparing activated carbon (Table 5, index 1) to ZrO_2 (index 2), TiO_2 (index 3), and Al_2O_3 (index 4) with 5 wt% Ru^0 and average NP diameters of ~1 nm. All of the oxide-supported catalysts yielded 81–86% FDCA. However, even at a lower Ru loading the Ru/C catalyst (40 : 1) achieved the highest yield of 97% compared to the oxide-supported catalysts (30 : 1).[87] Other metal oxide supports have also been used with Ru with increased oxygen availability being noted as a key component in effective HMF upgrading.[66] Zhang *et al.*[66] studied oxide supports containing Cu, Co, and Mg oxides and found that a 4 wt% Ru^0/Cu_xCo_yO catalyst with a 1 : 1 molar ratio of Cu : Co oxides (CuO and Co_3O_4; Ru/Cu1–Co1–O in Fig. 9) had a significantly lower FDCA yield than a 4 wt% Ru/MgO catalyst, which they attributed to a lack of basic sites. However, when using the Cu : Co support that was doped with 6 mmol of MgO, a yield of almost 80% FDCA was achieved (Ru/Cu1–Co1–O·MgO, Fig. 9) This mixture most effectively activated oxygen due to the synergistic effects between the Cu and Co oxides, with MgO playing a key role in structural effects. For the catalysts with Cu : Co ratios of 1 : 2 and 2 : 1, the FDCA yields were less than 40%, indicating that 1 : 1 was the optimum ratio. Running just the Cu1–Co1–O·MgO support resulted in only 3.5% FDCA, but 25.7% FFCA (Fig. 9), showing the need for Ru to drive the oxidation of HMF.[66]

When studying the effect of Ru loading on the Cu1–Co1–O·MgO support, Zhang *et al.*[66] evaluated the impact of 1–5 wt% Ru, which they had also studied previously on a Cr2–Fe1–O support with Ru loading ranging from 1–4 wt%.[75] In both studies, FDCA yields increased with Ru loading up to 4 wt% Ru, with yields of around 80% for the Cu1–Co1–O·MgO support[66] and near 100% with the Cr2–Fe1–O support (Fig. 10).[75] Increasing the Ru loading further to 5 wt% was hypothesized to result in an excess of Ru blocking pores and reducing surface area, allowing fewer active sites.[66] A different study that used Ru^0 on nitrogen-doped activated carbon catalysts saw a similar effect regarding the amount of Ru, with the highest amount of Ru resulting in lower FDCA yields (Ru/NC; Fig. 10).[88] In the 2023 study with the 4 wt% Ru/Cr2–Fe1–O catalyst, $KHCO_3$ was used as a liquid base, which led to high FDCA yields when 0.06 g was added, as previously mentioned (Table 5, index 5). Decreasing the amount of $KHCO_3$ to 0.04, 0.02, and 0 g resulted in FDCA yields of 54%, 30.3%, and 6.6%, respectively, verifying that the base additive was necessary when using the Cr2–Fe1–O supported catalyst.[75] A significant

Table 5 Ruthenium catalyst studied for aqueous HMF oxidation using 1 MPa O_2 at 100% HMF conversion

Index	Catalyst	Support	Base	t (h)	T (K)	$C_{HMF,i}$ (wt%)	HMF/Cat. (mol mol^{-1})	FDCA yield (%)	Ref.
1	Ru	C	$Mg(OH)_2$	8	383	0.5	40	97.3	87
2	Ru	ZrO_2	$Mg(OH)_2$	8	383	0.5	30	82.2	87
3	Ru	TiO_2	$Mg(OH)_2$	8	383	0.5	30	80.8	87
4	Ru	Al_2O_3	$Mg(OH)_2$	8	383	0.5	30	86.1	87
5	Ru	Cr2–Fe1–O	$KHCO_3$	16	373	0.5	5.1	99.9	75
6	Ru	N-doped C	$CaCO_3$	6	413	0.6	30	97	88
7	Ru	N-doped C	$CaCO_3$	2	413	0.6	30	45	88

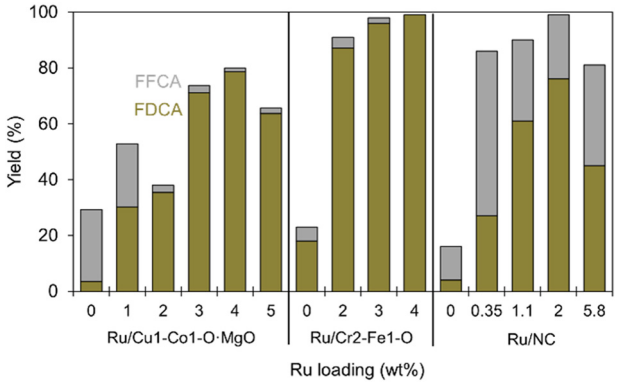

Fig. 10 The effect of Ru loading on FDCA (■) and FFCA (■) yields on a Cu1–Co1–O·MgO,[66] Cr2–Fe1–O,[75] and NC support.[88] Reaction conditions for Ru/Cu1–Co1–O catalyst: 0.5 wt% HMF, T = 383 K, P_{O_2} = 1 MPa O_2, t = 12 h,[66] for Ru/Cr2–Fe1–O catalyst: 6 mmol $KHCO_3$ additive, 0.5 wt% HMF, T = 373 K, P_{O_2} = 1 MPa, t = 16 h,[75] and for Ru/NC catalyst: 0.6 wt% HMF, 0.25 mmol $CaCO_3$ additive, T = 413 K, P_{O_2} = 1 MPa, t = 2 h.[88]

advantage of the Ru/Cu1–Co1–O·MgO catalyst was that no liquid base was required, eliminating potential HMF degradation as a result of alkalinity.[66]

In the case of the Ru/Cu1–Co1–O·MgO catalyst, the MgO was hypothesized to contribute the basic sites needed to complete conversion of HMF to FDCA. Zhang *et al.*[66] evaluated the effect of MgO loading and found that the FDCA yield increased up to 78.6% at 6 mmol MgO and then decreased at 8 mmol to near 40% (Fig. 11), which was attributed to a reduction of CuCo content, hampering catalytic activity.[66] The addition of Mg to Ru catalysts was found to assist in FDCA production not only as part of a support, but as a base additive as well. Another research group compared a wide range of base additives and found that $Mg(OH)_2$ resulted in the best mass balances and highest FDCA yields. The second most effective base, hydrotalcite (HT), also contained high amounts of Mg.[87] The exact mechanism by which Mg enhances furan oxidation has not been reported, but other alkaline earth metals such as Ca have been previously reported to enhance HMF oxidation reactions as well.[30] Regarding the amount of dopant added, Perumal *et al.*[86] made similar observations in their study of a Nb-doped Ru^0 catalyst supported by a mesoporous silicon structure, SBA-15. Increasing the amount of Nb improved FDCA yields up to 2.5 Nb atoms per 100 Si atoms, but increasing the loading further decreased FDCA yields (Fig. 11). The authors proposed that excess Nb dopant decreased surface effects and surface acidity, which negatively impacted furan conversion.[86] Using nitrogen as the dopant, Zhang *et al.*[88] also reported high yields over Ru NPs supported by a nitrogen-doped activated carbon, achieving 97% FDCA yield after 6 h of reaction time. (Table 5, index 6) This was significantly higher than the 45% FDCA yield achieved after 2 h (Table 5, index 7) even though the HMF conversion was 100%. Doping the carbon support with nitrogen improved electron density in the Ru NPs and prevalence of basic sites on the support. The increased electron density amongst the metal particles, particularly surface atoms, resulted in the transfer of 3d electrons to the π^* orbitals of O_2. Such a process weakened the oxygen–oxygen bond and primed the molecules for oxidation reactions.[88] The primary features of these carbon supports are their high surface areas, which have been observed across other noble metal catalysts,[58,75,79,86] the activation of O_2, and the stabilization of Ru NPs to guard against sintering.

Although most of the previously discussed HMF oxidation studies reported stable catalysts with minimal deactivation upon reuse,[66,75,86] a study by Mani *et al.*[25] reported the leaching of Mn under certain conditions for a Ru^0/MnO_2 catalyst. They studied multiple supports including MnO_2, $CoMn_2O_4$, $MnFe_2O_4$, and $CuOFe_2O_3$ and found that the MnO_2 catalyst resulted in the highest FDCA yields (91% compared to 82, 87, and 15%, respectively) and that higher initial HMF concentrations significantly decreased FDCA yields (Fig. 12). The decrease in yield was directly proportional to decreasing carbon balances, which was attributed to the low solubility of FDCA in the aqueous solution leading to precipitation of FDCA. After treating the 2 wt% HMF reaction

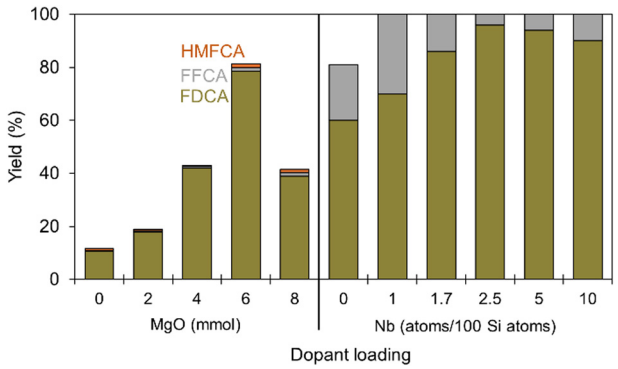

Fig. 11 Impact of dopant amount on FDCA (■), FFCA (■), and HMFCA (■) yields for a MgO dopant loaded on a 4% Ru/Cu1–Co1–O·MgO catalyst (100% HMF conversion for all)[66] and Nb loading on a Ru/SBA-15 catalyst.[86] Reaction conditions: P_{O_2} = 1 MPa, t = 12 h and for Cu1–Co1–O·MgO catalyst: 0.5 wt% HMF, T = 383 K,[66] and for Nb-SBA-15 catalyst: 1.25 wt% HMF, T = 393 K.[86]

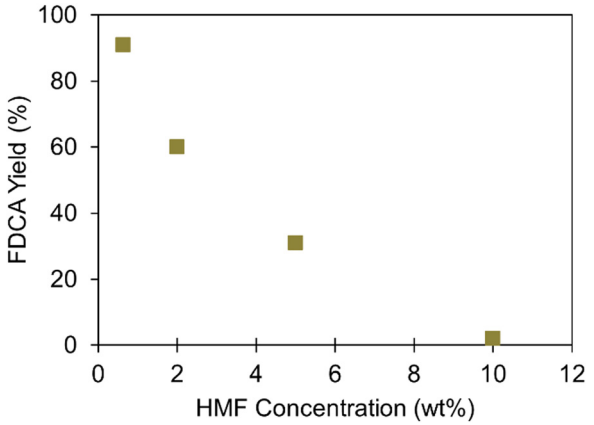

Fig. 12 Effect of initial HMF concentration on final FDCA yields observed in an aqueous system using a Ru/MnO_2 catalyst without the addition of base. Reaction conditions: 2 : 1 HMF : catalyst weight ratio, T = 373 K, P_{O_2} = 3 MPa, t = 24 h.[25]

effluent with base and an added organic solvent (MeOH), the FDCA yield increased markedly from 59% yield to 83%, indicating the presence of insoluble or precipitated FDCA that wasn't detected with the initial analysis. Also using 2 wt% HMF, the study found that Mn leached from the Ru/MnO_2 catalyst, which they attributed to the production of FDCA, an acidic product.[25] The stability of the catalyst in acidic medium is an important consideration if a base is not added to the reaction. FDCA has a relatively low $pK_a \pm 3$ which acidifies the medium as the reaction proceeds and, as reported by Mani *et al.*,[25] this effect is more pronounced at high HMF concentrations and can be a reason for catalyst deactivation due to metal leaching. When stoichiometric amounts of base ($NaHCO_3$) were added to the reaction, the amount of Mn detected significantly decreased from 988 ppm to 7 ppm, but small amounts of Ru (4 ppm) were also detected.[25]

Ruthenium catalysts, studied in aqueous systems as Ru^0, attained higher yields with smaller NP diameter, greater NP distribution, and higher catalyst surface area. However, for furan compounds to adsorb onto the catalyst surface and interact with these NPs, greater catalyst loading or surface area can become detrimental when it comes at the expense of sufficient pore sizes or active site availability. If excessive Ru NPs begin to block pores, it may restrict the access of reactants to the electron-dense catalyst. Dopants such as MgO or Nb are useful for improving Lewis acidic/alkaline properties, but the correct ratio of dopant to catalyst must be found for the best results. Accessibility of acidic or alkaline sites continues to be relevant, with the addition of bases being useful, but not necessary, for increased yields. To that end, weak bases containing Mg were found to be particularly effective at maintaining high mass balances and attaining high FDCA selectivity. The reason for this is not completely understood but could correlate to Mg's group (II) or its row on the periodic table since the addition of Ca in other reactions has been shown beneficial. Decreased initial HMF concentration was definitively shown to correlate to higher yields at constant reaction conditions.

Non-noble metal catalysts

Non-noble metals (NNM) such as Mn, Fe, Bi, Co, and Cu tend to be less active and less stable than noble metals; however, they have been extensively studied as catalysts because of their low cost and availability. NNMs, particularly first row metals (Mn–Zn), are easily oxidized in the presence of oxygen and these metal oxides can have their relative Lewis acidity change depending on surface adsorption. As such, NNM catalysts favor the HMFCA pathway (Schemes 3 and 5). The Mars–van Krevelen reaction mechanism is facilitated by oxygen atoms acting as Lewis acids. Additionally, oxygen vacancies in the metal oxide matrix generate strong Lewis base sites that attract water molecules. These water molecules react with the metal ion(s) surrounding the vacancy to complete the matrix, filling in the missing oxygen. This reaction mechanism can be tuned by replacing metal ions with a metal ion of a different valency or oxidation state.[89] This creates a change in the Lewis acid–base nature of the area and makes a catalytic hotspot where oxygen is either more easily exchanged with the adsorbed product or water can be more easily reacted with the resulting vacancy. There is a tradeoff, however; the easier a matrix oxygen atom is removed to oxidize a furan, the harder it is to replace the removed oxygen in the matrix and *vice versa*.[90,91] Another way to affect the catalytic potential of the metal oxide is by depositing metal on the surface. The deposited metal on the surface has its relative Lewis acidity promoted, and the metal also lowers the energy needed to form an oxygen vacancy in the immediate area.

Single metal non-noble catalysts

Few studies report the use of single metal NNM catalysts, as bimetallic catalysts take advantage of the different catalytic properties of the metals used. Using a zeolite support, Herlina *et al.*[92] impregnated ZSM-5 with NiO and CuO separately and reported that the optimal HMF oxidation temperature for these catalysts was 303 K using H_2O_2 as an oxidant. For the Ni-impregnated catalyst (Table 6, index 1), 79% FDCA yield was achieved after 5 h and for the Cu-impregnated catalyst (index 2), 70% FDCA yield was achieved compared to 50% FDCA with a non-impregnated ZSM-5 catalyst (index 3). The formation of oxides allowed the transition metals to have a higher oxidation state as both the Ni and Cu were held at a +2 oxidation state, which resulted in higher activity.[92]

Another way to increase the oxidation state of a NNM catalyst is by forming ligands. Chelating compounds trap and form ligands with metals, forcing them into a higher oxidation state and pulling electrons away from the metal atom. When in a higher oxidation state, the electronegative elements like oxygen are attracted to the less shielded nucleus. This allows water to adhere to the surface of the metal in the center of the chelate and oxidize, forming a hydroxide. This hydroxide can then interact with other molecules, causing them to oxidize as well.[93] Gao *et al.*[93] deposited iron tetraphenylphosphonium (FeTPP) to form a ligand on the surface of activated carbon

Table 6 Non-noble single metal catalysts studied for aqueous HMF oxidation

Index	Catalyst	Support	Base	t (h)	T (K)	P (MPa)	$C_{HMF,i}$ (wt%)	Oxidant	HMF/Cat. (mol mol^{-1})	HMF Conv. (%)	FDCA yield (%)	Ref.
1	NiO	ZSM-5	K_2CO_3	5	403	atm	3.6	H_2O_2	10	100	79	92
2	CuO	ZSM-5	K_2CO_3	5	403	atm	3.6	H_2O_2	10	80	70	92
3	—	ZSM-5	K_2CO_3	5	403	atm	3.6	H_2O_2	10	35	50	92
4	FeTPP-1	NC	NaOH	5	353	1	0.25	O_2	11	82	28	93
5	Co	NC-900	$NaCO_3$	12	338	0.5	0.12	O_2	0.024	100	82	94
6	Co	NC-900-a	$NaCO_3$	12	338	0.5	0.12	O_2	0.024	100	71	94
7	Co	NC-900-a	$NaCO_3$	16	338	0.2	0.52	O_2	0.12	100	94	94

and used this as the catalyst for HMF oxidation to form HMFCA. The iron chelates reacted to cyano-groups on the surface of the N-doped activated carbon rather than crystallizing on the surface. Using temperatures ranging from 333–373 K and higher concentrations of NaOH to stabilize the intermediate, the FDCA yield was 28% with 41% HMFCA (Table 6, index 4).[93]

Cobalt (Co) has also been investigated for HMF oxidation as a single metal catalyst. Y. Gao *et al.*[94] deposited Co on activated carbon, graphitized it, and achieved 81.8% FDCA yield (Table 6, index 5). They showed that Co NPs were the main catalytic site by acid etching away the surface Co and revealing previously carbon-bound Co sites, resulting in the NC-900-a catalysts (Table 6, indices 6 and 7). Using ICP, the concentration of Co on the unetched catalyst was 28.2%, while the concentration of Co after acid etching was only 0.71%. Using the etched catalyst resulted in a 16% decrease in FDCA yield after 12 h (Table 6, index 6) compared to the unetched catalyst. However, when using the same amount of the etched catalyst but 5 times the HMF (50 mM), a lower O_2 pressure, and increased reaction time of 16 h, 94% FDCA yield was achieved (Table 6, index 7).[94] Similarly to what was seen with Ru catalysts,[66] an excess of Co on the catalyst surface decreased the FDCA yield.

The Co catalysts used graphitized carbon as a support, a factor shown to influence FDCA yield. Gao *et al.* defined the degree of graphitization as the ratio of random, unorganized carbons (D peak in Raman spectroscopy; I_D) divided by the number of organized or graphitic carbons (G peak in Raman spectroscopy; I_G).[94] The degree of graphitization that resulted in the highest FDCA yield was determined to be 0.6 for the etched Co-catalyst and 0.7 for the unetched (Fig. 13). The acid etching of the Co/NC-900-a catalyst reportedly removed some of the disorganized carbon, leading to a higher ratio of graphitized carbon that had a higher surface area,[94] which could be the reason there was not a large decrease in the catalytic activity after much of the surface Co was removed.

Bimetallic non-noble catalysts

Single metal NNM catalysts have been shown to be effective for the oxidation of HMF to FDCA, but using bimetallic catalysts can greatly increase catalytic activity. When using two oxides of differing charge densities, the effects of the individual metals can be amplified by being chemically bonded to each other. For example, Cu oxide is a strong oxidizing catalyst but has little selectivity, while Co has high selectivity but lower activity.

Rao *et al.*[95] compared Cu and Co at two different oxidation states each, Co and Cu oxides physically mixed, and a CuO_x–CoO_y nanoparticle both randomly deposited and organized using polyvinylpyrrolidone (PVP) as catalysts for HMF oxidation. Using the same reaction conditions, all catalysts achieved high HMF conversion (greater than 95%), but the FDCA yields varied significantly (Fig. 14). The Cu oxides achieved a maximum FDCA yield of 39%, while the Co oxide achieved 54%. Using both the CuO_x and CoO_x together as a physical mixture resulted in 55% FDCA yield, but with a one-pot synthesis method using both Cu and Co oxide, the FDCA yield increased to 67% showing the enhancement of properties using both oxides. Rao *et al.* also deposited the Cu–Co oxide catalyst onto graphite and the FDCA yield increased to 80%, while using PVP to organize the structure on the surface of graphite increased the FDCA yield to 91%.[95] Separately, both Cu and Co were active catalysts, but when combined into a single metal oxide, both of their catalytic properties were enhanced, leading to higher selectivity.

This higher selectivity and conversion could be due to the ability of CoO to form H_2O_2 in the presence of water and O_2. Zhang *et al.* (2024)[96] looked at Cu–Co oxide catalysts as well but focused on the oxygen being added to the reaction media. They found that under alkaline conditions, CoO could reduce O_2 to hydrogen peroxide. This was observed in Cu–Co oxide catalysts as well. They then showed that Cu could oxidize the H_2O_2 into copper peroxide. This copper superoxide would then be reduced by a furan, causing the furan to oxidize.[96]

Cobalt has been used with other metal oxides as well. Zang *et al.*[97] used a bimetallic Co and bismuth (Bi) oxide catalyst since pure Bi oxide converted 98% HMF but resulted in little FDCA yield (Table 7, index 1). The results using Co oxide were

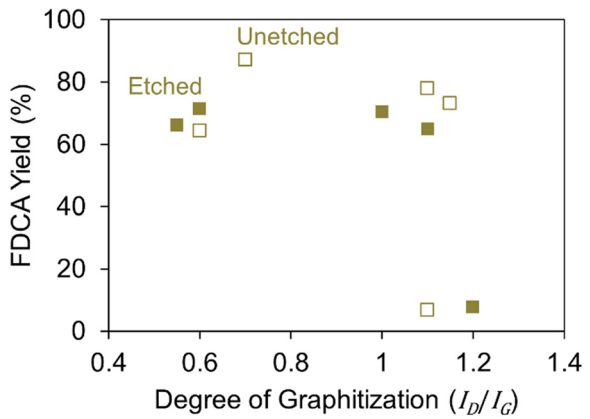

Fig. 13 The effect of graphitization on FDCA yields. Reaction conditions: 0.024 HMF : catalyst molar ratio, T = 338 K, P_{O_2} = 0.5 MPa, t = 12 h.[94]

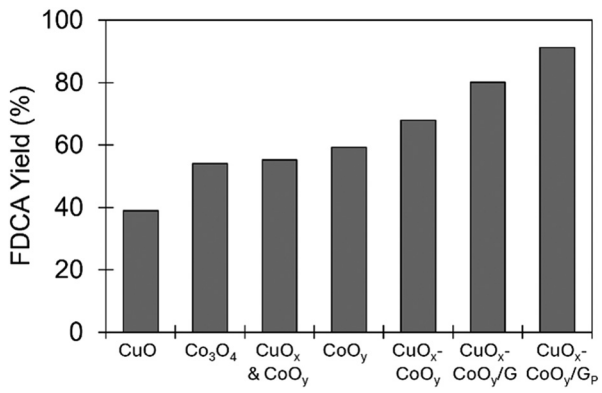

Fig. 14 FDCA yields of various Cu- and Co-based catalysts where G represents graphite deposited catalysts and G_P represents the PVP-organized catalyst on graphite. All HMF conversions were greater than 95%. Reaction conditions: 0.525 : 1 HMF : catalyst by wt, 3.2 mmol NaClO, 0.5 mmol HMF, T = 303 K, P = atm, t =1 h.[95]

Table 7 Non-noble bimetallic catalysts that have been studied for aqueous-based HMF oxidation with NaOH as a base additive

Index	Catalyst	Support	t (h)	T (K)	P_{O_2} (MPa)	$C_{HMF,i}$ (wt%)	HMF/Cat. (mol mol^{-1})	HMF Conv. (%)	FDCA yield (%)	Ref.
1	Bi_2O_3	—	3	383	0.6	0.083	0.17	97	0.5	97
2	Co_3O_4	—	3	383	0.6	0.083	0.05	100	20	97
3	12 Co : Bi	—	3	383	0.6	0.083	0.06	99.9	98.2	97
4	10%Bi–CeO_2	—	12	383	1	0.14	0.21	98	30	22
5	10%Bi–CeO_2	NC-800C	12	383	1	0.14	0.14	100	55	22

better with 100% HMF conversion and 20% FDCA yield (Table 7, index 2), but using these same conditions and a binary metal oxide consisting of 12 mol% Bi and the remainder Co (CoBi-12), the FDCA yield increased to 98.2% at 100% HMF conversion (index 3).[97] This Co–Bi catalyst was an improvement on previous work using Bi and cerium (Ce) oxide that achieved 30% FDCA yield at 100% HMF conversion (Table 7, index 4).[22] However, similar to Rao *et al.*,[95] when Wei *et al.*[22] deposited the Ce–Bi metal oxide on activated carbon, which increased the surface area, raising the FDCA yield from 30% to 55% using only 1.6 mmol NaOH (Table 7, index 5). Zhang *et al.*[97] also studied the effect of alkalinity on the production of FDCA using the CoBi-12 catalyst by increasing the amount of NaOH with respect to initial HMF concentrations. They found that a molar ratio of 2 : 1 NaOH to HMF was optimal, resulting in near ideal selectivity of 98% FDCA (Fig. 15). Increasing the NaOH ratio further resulted in decreased FDCA yields, likely due to HMF degradation as mentioned previously.

As single-metal non-noble catalysts, transition metal oxide catalysts typically have low effectiveness in aqueous systems. However, increasing the surface area of the catalyst significantly improves the activity of the catalyst. A consideration when using carbon-based supports is that having graphitic carbon on the surface increases the effectiveness of the catalyst but tends to reduce the surface area. Metal oxide catalysts also greatly benefit from the addition of another transition metal oxide. These mixed metal oxides amplify the properties of both individual metals rather than just averaging out the two oxides' properties.

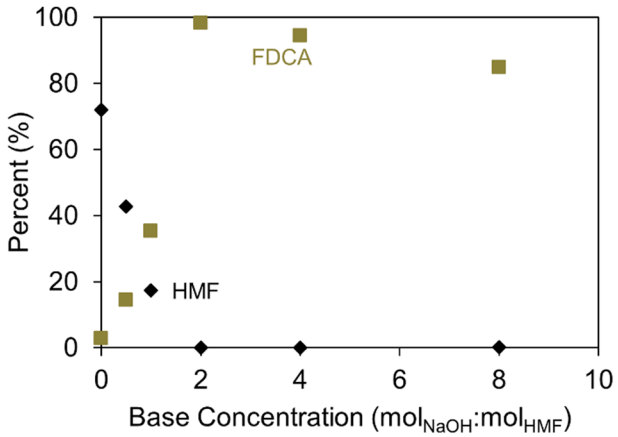

Fig. 15 The effect of NaOH on HMF conversion (♦) and FDCA yield (■) using a Co–Bi oxide catalyst. Reaction conditions: 0.056 HMF : catalyst molar ratio, 0.8 mmol of NaOH, T = 380 K, P_{O_2} = 0.6 MPa, t = 3 h.[97]

Organic solvent reactions

Using water as a solvent results in high HMF conversion and FDCA selectivity typically at low HMF concentrations. However, there are several reasons to consider using organic solvents as the reaction medium for the HMF to FDCA reaction. First, economic and sustainable production of FDCA is linked to the production of HMF, which is produced from the dehydration of C_6 sugars in acidic medium.[17,98–101] An important consideration is that in the presence of water and acid catalyst, HMF reacts to produce levulinic and formic acid and can polymerize to form humins. To avoid HMF degradation, biphasic and/or organic monophasic systems have been used, so that the HMF is extracted and produced in an organic solvent.[54,102–105]

Another important reason to study the oxidation of HMF in organic solvents is to increase FDCA solubility, as concentrations around 10 wt% are necessary to consider the process industrially relevant.[106] In order to improve FDCA solubility, many solvent blends involving water and an additional organic solvent have been studied[35,36,52,107,108] with researchers showing that organic solvents can solubilize up to 31 wt% FDCA compared to 0.12 wt% in water at STP.[34] However, solvents must also be stable at the reaction conditions, offer a sufficient source of oxygen for reaction progress, and not interact with furan compounds in such a way that hinders the oxidation process. These issues can be mitigated by selecting an organic solvent or blend of solvents with the correct physical and chemical characteristics to promote both solubility and reaction progress.

In the case of solvent interactions, several research groups have discussed the importance of solvent selection in HMF to FDCA reaction design.[52,109,110] As shown in Scheme 1, furan compounds contain carbonyl (C═O) and alcohol (O–H) groups, which are capable of forming hydrogen bonds with organic solvents, both as hydrogen bond donors (O–H) and acceptors (C═O). There are multiple ways to measure solvent properties for evaluation; two options that have been used previously are the Hansen Solubility Parameters (HSPs)[34,108] of hydrogen bonding (δ_H), dispersion (δ_D), and polarity (δ_P),[111] and the Kamlet–Abboud–Taft (KT) parameters[52] of hydrogen bond acceptor basicity (β), hydrogen bond donor acidity (α), and polarizability (π*).[112] In particular, hydrogen bond contribution and polarity have been identified to be of interest for HMF oxidation. The hydrogen bond contribution has been shown to positively impact the capacity of a solvent to solubilize FDCA, but can also negatively impact the forward progress of HMF oxidation through strong solvent–reactant intermolecular interactions with intermediates.[52] Polarity impacts reaction progress

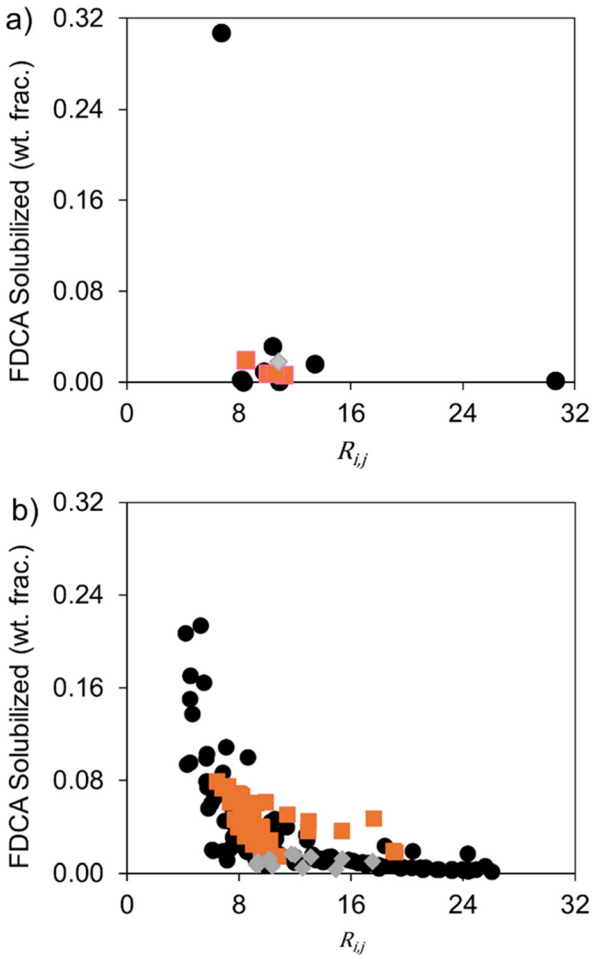

Fig. 16 Relationship between the $R_{i,j}$ parameter and FDCA solubility in (a) pure solvents and (b) binary aqueous/organic mixtures and ternary aqueous/organic/organic mixtures from (●),[34] (■),[108] and (♦).[35]

by facilitating the dissolution of oxygen and HMF conversion.[109] Additionally, a holistic parameter, the radius of interaction ($R_{i,j}$), compares all the HSPs of the solute (i; FDCA in this case) to the solvent (j) and has been identified to show a strong correlation between the maximum FDCA solubility and the minimum $R_{i,j}$ of a solvent.[34] This trend was found to be weak for pure solvents, as demonstrated in Fig. 16a, but was significantly stronger in aqueous/organic solvent blends (Fig. 16b).

These variables of interest are listed in Table 8 for a range of organic solvents that have been reported in the literature, including γ-valerolactone (GVL),[34,36,52] dimethyl sulfoxide (DMSO),[34,52] acetonitrile (ACN),[26,34] *tert*-butyl alcohol (TBA),[50] 1,2-dimethoxyethane (DME), diglyme (DG), and 1,4-dioxane (DX).[52,54] Additionally, other studies mention improved solubility in dimethylformamide (DMF), ethanol (EtOH),[113] methanol (MeOH), acetone (ACE),[53] *n*-propanol (*n*-PrOH), and isopropanol (i-PrOH)[109] without reporting pure solvent FDCA solubilities.

Pure DMSO had the highest reported FDCA solubility of over 30 wt% at 293 K (Table 8),[34,52] which was attributed to the strong dipole–dipole interactivity of DMSO and its high capacity for hydrogen bond acceptance.[117,118] It is worth noting that Table 8 lists the FDCA solubility for the pure solvent, and not for aqueous/organic blends, which in most cases achieved higher FDCA solubilities. For example, FDCA solubility was shown to increase nearly four-fold in binary mixtures of water and DX compared to the pure solvent, which was attributed to the hydroxyl groups on FDCA acting as Lewis acids or hydrogen bond contributors, while the carbonyl groups can function as hydrogen bond acceptors.[108] The correlation between FDCA solubility and ability of a solvent to hydrogen bond was noted to be true across all ether-type solvents and solvent blends and can largely be extended to other solvent types as well, with correlation made most strongly to the KT β parameter.[52] Additionally, FDCA solubility has also been shown to correlate with an increased heat of mixing (ΔH_{mix})[36] and a lower $R_{i,j}$ (Fig. 16).[34]

However, high FDCA solubility is not the only consideration, as ideally the solvent would also promote HMF oxidation. In some cases, solvents have high FDCA solubility, but low FDCA yields due to interactions of the solvents with the reactant and/or intermediates.[52] For example, DMSO is of great

Table 8 Overview of properties and FDCA solubility at 303 K[a] or 293 K for various solvents

Solvent	Pure solvent FDCA solubility (wt%)	KT hydrogen bond acceptor (β)[d]	KT hydrogen bond donor (α)[d]	HSP hydrogen (δ_H)[e]	HSP polarity (δ_P)[e]	HSP $R_{i,j}$
DX	0.42[a]	0.37	0.00	9.0	1.8	7.8
DME	0.3[b]	0.41	0.00	4.9	4.9	12.9
TBA	—	0.93	0.42	14.7	5.1	10.0
DG	0.3[b]	0.40	0.00	6.5	6.1	10.6
i-PrOH	—	0.84	0.76	16.4	6.1	9.0
n-PrOH	—	0.90	0.84	17.4	6.8	8.9
EtOH	0.92[c]	0.75	0.86	19.4	8.8	9.8
ACE	—	0.43	0.08	7.0	10.4	9.8
MeOH	1.59[c]	0.66	0.98	22.3	12.3	13.4
DMF	23.0[b]	0.69	0.00	11.3	13.7	5.5
H_2O	0.12[c]	0.47	1.17	42	16	30.6
DMSO	30.7[c]	0.76	0.00	10.2	16.4	6.7
GVL	0.19[c]	0.58	0.00	6.7	16.5	5.9
ACN	0.02[c]	0.40	0.19	6.1	18.0	10.6

[a] Xu *et al.*[114] [b] Ryu *et al.*[52] [c] Molinaro *et al.*[34] [d] R. Stenutz.[115] [e] HSPiP Software Package.[116]

interest for application in HMF upgrading due to its high capacity to solubilize furan compounds. However, Fourier-transform infrared analysis (FTIR) studies on HMF-DMSO pairings showed DMSO interacts strongly with both the alcohol and carbonyl groups of HMF through hydrogen bonding and dipole – induced dipole effects, limiting reaction progress beyond DFF. The tendency of DMSO to interact strongly with the furanic solute molecules resulted in reduced capacity for oxidants and catalysts to facilitate reaction progress. Similarly, in the case of GVL, strong interactions with the C=O groups in DFF and FFCA limited forward progress to FDCA.[52] This trend of organic solvents interacting with the C=O and O–H groups of HMF and DFF and having limited selectivity to FFCA or FDCA has also been reported elsewhere in the literature.[109,113]

Additionally, consideration of the stability of the organic solvent is important. A common organic solvent, tetrahydrofuran (THF), is not regularly applied in HMF oxidation reactions despite a relatively high FDCA solubility of 3.2 wt% at STP[34] because of its tendency to convert to γ-butyrolactone (GBL). In a reaction with a $ZnFe_2O_4$ catalyst at 353 K, nearly 50% of the THF converted to GBL in 12 h.[119] Other solvents are more resistant to reaction, such as GVL, for example. At 373 K and in acidic conditions, GVL was found to reach equilibrium after the formation of only 4 mol% 4-hydroxyvaleric acid (4-HVA) as a side product.[120] Although it would be most desirable to have no solvent react, minimizing its degradation should be a key consideration.

Based on the solubility and process benefits of organic and aqueous/organic solvent systems, there has been a recent influx of publications focusing on the use of organic reaction media for HMF oxidation. In the following sections, the impact of solvent, catalyst type, and reaction conditions will be discussed to determine key trends for improving HMF conversion and FDCA yields in organic solvent systems.

Noble metal catalysts

As in aqueous systems, the application of the noble metals Pt, Pd, Au, and Ru as catalysts for HMF upgrading has been commonly reported. Since Prasad *et al.* completed their review in 2023,[48] several papers have focused on noble metal catalysis in organics and show similar trends to those observed in aqueous systems described previously, including improved FDCA yields using catalysts containing the metallic (zero-valence state) forms of metals, those with increased oxygen content, and those with smaller diameter particles that are more evenly distributed across the surface of the catalyst.

Both Ryu *et al.*[52] and Motagamwala *et al.*[36] used Pt^0 for reactions run in organic solvents. Ryu *et al.*[52] found that the overall product selectivity remained low and FDCA yields remained below 30% in pure solvents including DMSO (0%), DMF (0%), GVL (0.7%), DG (27%), DME (6.9%), and DX (1.4%) (Table 9, indices 1–6).[52] Low selectivity towards FDCA in pure organic solvents relates to prior discussion of solvent-reactant intermolecular interactions, particularly corresponding to hydrogen bond acceptance (β). In the study by Ryu *et al.*, DMSO, DMF, and GVL have high β values relative to the other solvents (Table 8) and decreasing β values corresponded to increasing HMF conversion and, in the case of any FDCA production at all, increasing FDCA production (Table 9, indices 1–6).

Although some FDCA yields were seen with pure organic solvents, using aqueous mixtures of organics led to higher FDCA yields. In a separate study by Motagamwala *et al.*,[36] they used a Pt/C catalyst, 80/20 w/w GVL/water, and low concentrations of HMF (0.5 wt%) to achieve 95% FDCA yield (Table 9, index 7). However, when the HMF concentration was increased to 5 wt%, the FDCA yield decreased to 11% (Table 9, index 8). They determined that the 80/20 w/w GVL/water solvent did not have sufficient water to provide oxygen to facilitate the formation of the intermediate geminal diol.[36] However, using a 50/50 w/w GVL/water solvent blend and an HMF concentration of 7.5 wt% resulted in FDCA yields near 95% (Table 9, index 9), highlighting the need for sufficient water to be present in organic solvents.[36]

Using a solvent with low hydrogen bond acceptance (β) capacity and low polarity, Chen *et al.*[54] investigated a Ru/C catalyzed system in 50/50 w/w DX/water. Binary mixtures of DX and water have been previously shown to address solubility concerns,[52,108,114] while the lack of solvent–reactant interactions was proposed to be beneficial for the two-step upgrading of fructose to FDCA. As mentioned previously, the two-step process with first upgrading the sugar to HMF and then further converting to FDCA in the same solvent would be beneficial. Chen *et al.*[54] consistently achieved fructose to HMF yields of approximately 90% in 85/15 w/w DX/water before extracting the HMF and diluting to 3.15 wt% HMF in 50/50 DX/water. The resulting oxidation saw 100% HMF conversion with an 89% selectivity to FDCA (Table 9, index 10).

Table 9 Noble metal catalysts on carbon supports studied in organic solvent systems for HMF oxidation

Index	Catalyst	Solvent (w/w)	t (h)	T (K)	P_{O_2} (MPa)	$C_{HMF,i}$ (wt%)	HMF/Cat. (mol mol^{-1})	HMF Conv. (%)	FDCA yield (%)	Ref.
1	Pt	DMSO	2.5	393	1	1	50	2.6	0	52
2	Pt	DMF	2.5	393	1	1	50	5.1	0	52
3	Pt	GVL	2.5	393	1	1	50	78.9	0.7	52
4	Pt	DG	2.5	393	1	1	50	82	27	52
5	Pt	DME	2.5	393	1	1	50	93.2	6.9	52
6	Pt	DX	2.5	393	1	1	50	86.8	1.4	52
7	Pt	GVL/H_2O (80/20)	20	383	4	0.5	15	97	95	36
8	Pt	GVL/H_2O (80/20)	20	383	4	5	20	100	11	36
9	Pt	GVL/H_2O (50/50)	20	383	4	7.5	30	100	94	36
10	Ru	DX/H_2O (50/50)	12	393	1	3.2	15.8	100	89	54

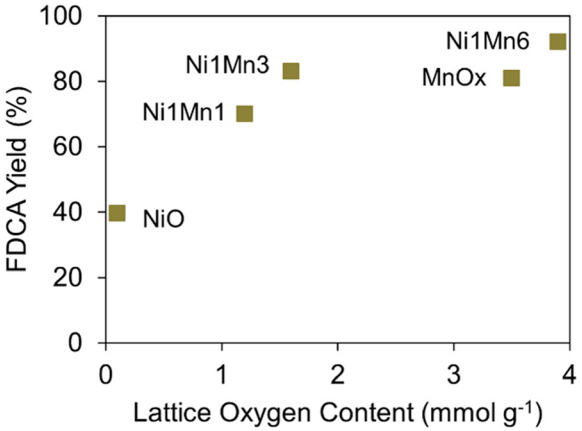

Fig. 17 Effect of lattice oxygen content of Ru catalysts supported by a range of Ni–Mn supports on FDCA yield at an HMF conversion of 100% (excluding Ru/NiO where the HMF conversion was 63%). Reaction conditions: 1.43 : 1 catalyst : HMF by weight; 70/30 H2O/ACE w/w; 5 wt% initial HMF; T = 383 K; P_{O_2} = 1 MPa; t = 12 h.[53]

While many researchers have reported high HMF conversion and FDCA selectivity over Pt and Ru single metal catalysts, research has also been done on bimetallic catalysts. Rao *et al.*[53] studied Ru-doped Ni–manganite catalysts and found that higher Mn content facilitated the formation of Ru^{3+} and Ru^{4+} *versus* higher ratios of Ru^0 at lower Mn content.[53] The catalyst with the most manganese-rich support, Ru/Ni_1Mn_6, had increased oxygen content, which led to higher oxidative activity and yields of FDCA (Fig. 17). Similar findings were also reported by Qian *et al.*[121] when studying non-noble bimetallic catalysts containing Ni and Co, which will be discussed in more detail in the NNM catalyst section below.

Rao *et al.*[53] found that metal surface area, as determined using CO-chemisorption, positively correlated with FDCA yields (Fig. 18a) while Ru particle size negatively correlated (Fig. 18b). Particle dispersion was also measured and observed to positively correlate with greater selectivity to FDCA. The support that resulted in the highest yield (92%), Ni_1Mn_6, had 72% dispersion of Ru NPs, compared to 53% dispersion on the next most active support, Ni_1Mn_3.[53] As with aqueous reactions, increased surface area and decreased particle size were seen to improve catalytic activity for a given type of catalyst.

Trends amongst noble metal catalysts using organic and aqueous/organic solvent systems paralleled those observed in purely aqueous systems. Correlations were found between increased FDCA yields and decreased active particle size, increased particle dispersion, and increased lattice oxygen content. The catalyst surface area improved FDCA yields, but only within a given catalyst design. The addition of organic solvents to the reaction system impacted product selectivity through interactions with furan intermediates like DFF and HMFCA, primarily *via* hydrogen bond formation at high concentrations of organic solvent. Improved solubility of furans through the addition of organics also allowed for high FDCA yields at initial HMF concentrations greater than 5 wt%.

Non-noble metal catalysts

As was true for aqueous systems, NNM catalysts are of increasing interest in organic and organic/aqueous systems. Though generally less active than NM catalysts, metals like Co, Fe, Cu, V, Mn, and Ni are lower in cost and more readily available, potentially providing new paths to commercialization for a process limited by its economic feasibility. This is particularly true in conjunction with the use of organic solvent systems, combining lower cost metal catalysts with the capacity for operating at higher HMF concentrations. From a broad perspective, NNM catalysts can form many different valence states (Table 10), and such versatility lends itself well to bimetallic catalysts, oxide catalysts, and other unique catalytic approaches that are not possible with noble metals. A wide range of NNM catalysts have been studied on a variety of supports and in different solvents blends, showing several of the same trends that were observed in water.

Similar to aqueous phase reactions, bimetallic NNM catalysts have more activity compared to single-NNM catalysts. Four recent studies used single-metal NNM catalysts as controls to study bimetallic catalysts, and the bimetallic catalysts consistently

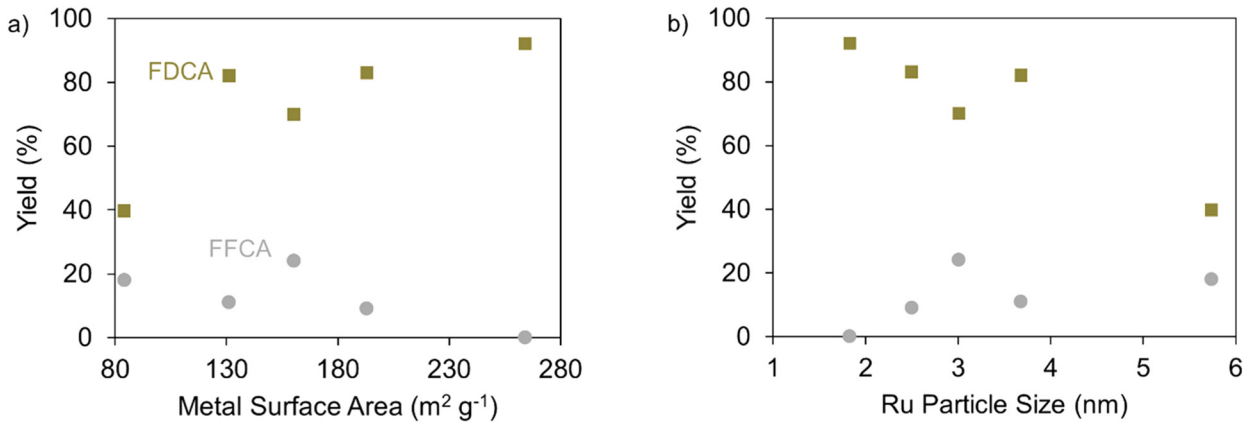

Fig. 18 Comparison of the effect of catalyst (a) metal surface area and (b) Ru particle size on an HMF oxidation reaction. Reaction conditions: 1 : 1.43 HMF : catalyst by weight, 70/30 w/w water/ACE, 5 wt% initial HMF, T = 383 K, P_{O_2} = 1 MPa, t = 12 h.[53]

Table 10 Oxidation and electron orbital configurations of different non-noble metals

Metal	Possible oxidation states	Electron orbital configuration
V	+2, +3, +4, +5	[Ar] $3d^3$ $4s^2$
Mn	+2, +3, +4, +6, +7	[Ar] $3d^5$ $4s^2$
Fe	+1, +2, +3, +4, +5, +6	[Ar] $3d^6$ $4s^2$
Co	+1, +2, +3, +4, +5	[Ar] $3d^7$ $4s^2$
Ni	−1, 0, +1, +2, +3, +4	[Ar] $3d^8$ $4s^2$
Cu	+1, +2, +3, +4	[Ar] $3d^{10}$ $4s^1$

outperformed the single metal catalysts with respect to both HMF conversion and FDCA yield.

For example, Demet *et al.*[26] studied a range of atomic metal ratios for both Mn–Cu and Fe–Co catalysts in a pure ACN solvent system. The pure metals, shown at either end of Fig. 19, represent FDCA yield minima for all bimetallic systems. For bimetallic systems, FDCA yields increased to nearly 30% for the Mn–Cu catalyst and nearly 25% for the Fe–Co catalyst. When present in smaller proportions relative to the less charged component, the more highly charged metal–Mn in the Mn–Cu system (Mn^{3+}/Mn^{4+}) and Fe in the Fe–Co system (Fe^{3+})-produced higher yields.[26] Liu *et al.*[113] saw that the pure metal catalysts of Cu and VO on a nitrogen-containing polymer support (PDVTA) had high FDCA yields of approximately 61 and 78% in a DMSO/TBA solvent, respectively (Fig. 19). Similar to the other catalysts presented in Fig. 19, when a bimetallic catalyst was used, FDCA yields were higher, and in the case of Cu–VO/PDVTA, FDCA yields were almost 90%. The authors attributed this increased yield to the synergistic effects of the two metals.[113]

The disparity in activity between two Cu bimetallic catalysts[26,113] highlights the importance of both the secondary metal and the support. The catalysts studied by Demet *et al.*[26] were unsupported, acting as mixtures of metallic oxides rather than as deposited particles on a support like those prepared by Liu *et al.* The PVDTA support allowed for an increase in particle dispersion,[113] a factor previously observed to impact catalyst activity by Rao *et al.*[53] The use of VO as a secondary metal may have also impacted the activity of the catalyst for similar reasons as those discussed regarding bimetallic Au catalysts; primarily, factors such as electron density, reactivity, and reactant adsorption capacity.

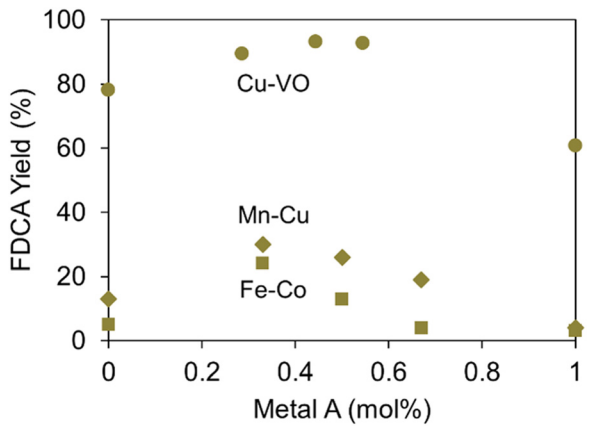

Fig. 19 Comparison of FDCA yields on single metal and bimetallic catalysts containing Mn–Cu (♦), Fe–Co (■),[26] and Cu^{2+}–VO^{2+} over a PVDTA support (●).[113] Reaction conditions for the Mn–Cu and Fe–Co catalysts: 1 : 4 HMF : catalyst by weight, pure ACN, 13 : 1 TBHP : HMF molar ratio, 3.5 wt% initial HMF, T = 333 K, P = atm, t = 3 h,[26] and for the Cu–VO/PVDTA catalyst: 32/68 w/w DMSO/TBA, 0.37 wt% initial HMF, T = 363 K, P = atm, t = 5 h.[113]

Yang *et al.*[50] also studied Mn, Cu, and V catalysts, varying the supports across a range of MoO_3 polymorphs in a TBA solvent. Like Liu *et al.*,[113] they found that the V-doped catalyst had the highest FDCA yields, also correlating both surface area (Fig. 20a) and pore volume (Fig. 20b) to these high yields. The high activity of the catalyst was further attributed to a balance of acidic and basic sites due to the incorporation of V onto the support, and the structure of the support itself. The polymorph of MoO_3 had a significant effect on both the HMF conversion and the FDCA yields, with α-MoO_3 having the highest activity as a catalyst without the addition of metal, but FDCA yields were only around 30% (Fig. 20a). This was attributed to the [010] crystal plane of α-MoO_3 being favorable for contact with the substrate.[113] The same correlations to surface area and pore size held true for the non-doped supports as were seen on the metal-doped catalysts (Fig. 20b).[50]

The importance of basic sites to facilitate HMF conversion observed by Yang *et al.*[50] was also noted by Liu *et al.*[113] and Hameed *et al.*[28] In the first case, basic amine groups at the surface of the catalyst helped to coordinate metal ions (Cu^{2+} and VO^{2+}) and improve catalytic efficiency.[113] In the second case, a Fe–N–C catalyst was supported on a range of metal oxides that led to a range of Lewis acid–base chemistries present at the surface of the catalysts, with Al_2O_3 leading to the highest FDCA yield (99.8%) and MgO the lowest (7.5%). NH_3-TPD analysis showed increasing intensity of acidic sites in the order of MgO < ZrO_2 < TiO_2 < Al_2O_3 (Fig. 21), while CO_2-TPD analysis showed an increasing intensity of basic sites in identical order.[28] Another study by Zheng *et al.*[87] also reported the highest yields of FDCA for their Ru-based system over an Al_2O_3 support.

Hameed *et al.*[28] also highlighted the catalytic importance of nitrogen in the catalyst structure, emphasizing its ability to exhibit electron-withdrawing and donating effects. Nitrogen atoms acted as the primary ligands by which the single-atom Fe catalyst, operating in 50/50 w/w DMSO/H_2O, was attached to a carbon backbone. Furthermore, the nitrogen stabilized the Fe into a higher valence state, Fe^{5+}, than would typically be observed through formation of FeN_5 structures. These penta-coordinated structures were hypothesized to be the most active part of the catalyst, generating active oxygen species for the conversion of HMF towards FDCA.[28] Rao *et al.*[23] also upgraded HMF over a N-doped catalyst, a carbonized bamboo sawdust catalyst doped with melamine as a nitrogen source using MeOH as the solvent. The lack of metal in the catalyst allowed for a more direct study of the impact of nitrogen on the catalyst structure and activity at a range of carbonization temperatures (873–1173 K). Pyridinic, pyrrolic, and graphitic nitrogen were all observed in the catalyst structures, at varying concentrations

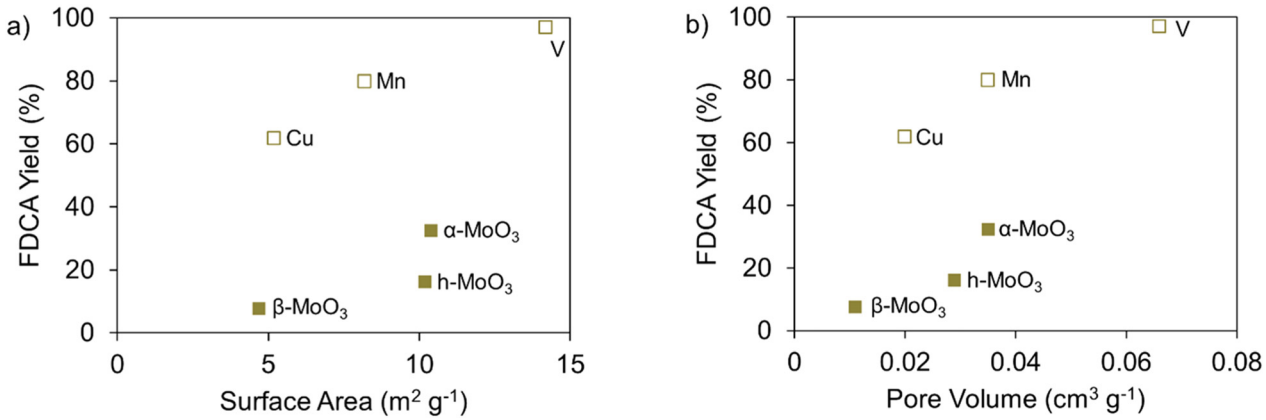

Fig. 20 The relationship between FDCA yield and (a) surface area and (b) pore volume for NNM catalysts on α-MoO_3 supports (□) and different MoO_3 phases without additional metal (■) (reaction conditions: 4 mL TBA solvent, 4 mmol TBHP, 0.4 wt% HMF, T = 353 K, P = atm, t = 12 h).[50]

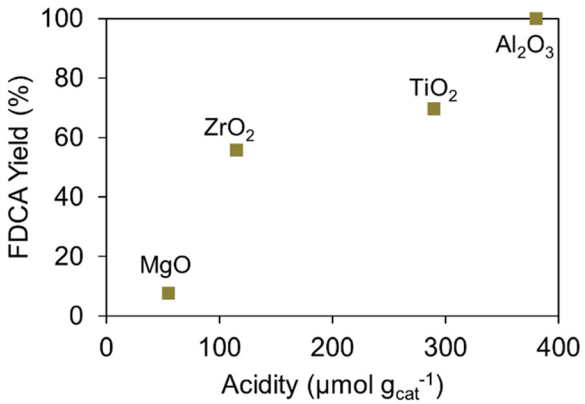

Fig. 21 Relationship between catalyst surface acidity and FDCA yield. Reaction conditions: 30 : 1 HMF : catalyst molar ratio, 50/50 w/w DMSO/water, 0.95 wt% HMF, T = 383 K, P = atm, t = 15 h.[28]

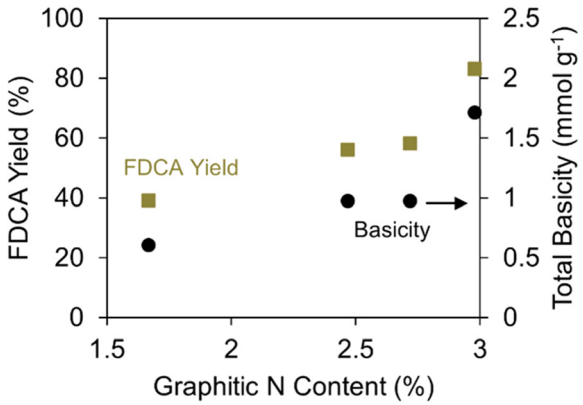

Fig. 22 Impact of graphitic N content on FDCA yield (■) and total catalyst basicity (●). Reaction conditions: MeOH solvent, 0.1 M K_2CO_3 weak base additive, 0.89 wt% HMF, T = 433 K, P_{O_2} = 2 MPa, t = 6 h.[23]

dependent upon the carbonization temperature. While no correlation was observed between the presence of pyridinic or pyrrolic nitrogen content, increased abundance of graphitic nitrogen did correlate to both increased presence of acidic and basic sites as well as increased yields of FDCA (Fig. 22).[23]

Gao *et al.*[27] also reported improved yields due to an increased availability of basic sites while investigating Co–Fe catalysts supported by hydrotalcite doped with either sulfur (S) or phosphorous (P). While layered double hydroxide (LDH) supports are more commonly applied in electrocatalytic systems,[122,123] where they excel due to their tunable redox properties, their use in thermochemical oxidation also shows high HMF conversions and FDCA yields. Distribution of Co and Fe on the LDH hydrotalcite support allowed for improved electron transfer ability between $Co^{2+/3+}$ and $Fe^{2+/3+}$, particularly with the introduction of S or P dopants. The addition of these non-metal elements created three-dimensional structures in the LDH, increasing catalyst surface area, pore diameter, and pore volume.[27] These physical attributes were maximized for the catalyst with the highest FDCA yield, a P-doped Co–Fe/LDH catalyst (Co–Fe–P-400/LDH) that converted 98% of HMF with 61% selectivity to FDCA in ACN (Table 11, index 1). When studying reaction temperature, the difference in catalytic activity between the S- and P-doped catalysts was similar (Fig. 23), suggesting that both S- and P-doping had similar effects and that the enhanced catalytic activity correlated more strongly to the availability of basic sites.[27]

Using the CoFeP-400/LDH catalyst, Gao *et al.*[27] studied the oxidation of HMF in several different solvents including ACN, DMF, DMSO, and EtOH (Table 11, indices 1–4). As had been observed by Ryu *et al.*,[52] the molecular properties and interactivities of the solvent impacted the distribution of products obtained from HMF oxidation. In this selection of solvents, the effect of hydrogen bond acceptance capacity was less clear. The solvent with the lowest β value, ACN (0.4), achieved the highest HMF conversion and FDCA yield. In contrast, DMF, DMSO, and EtOH, with β-values ranging from 0.69–0.76 (Table 8), were more selective towards primary intermediates like HMFCA.[27] However, these three solvents did not follow a clear trend in HMF conversion (Fig. 24a) as data presented by Ryu *et al.* had, where lower β values corresponded to further reaction progress.[52] For example, DMF (β = 0.69) had 42% HMF conversion,

Table 11 Non-noble metal catalysts studied in organic solvent systems for HMF oxidation at 353 K

Index	Catalyst	Support	Solvent	t (h)	$C_{HMF,i}$ (wt%)	HMF/Cat (mol mol^{-1})	HMF Conv. (%)	FDCA yield (%)	Ref.
1	Co–Fe–P-400	LDH	ACN	6	0.61	NR	98	60	27
2	Co–Fe–P-400	LDH	DMF	6	0.51	NR	42	4.2	27
3	Co–Fe–P-400	LDH	DMSO	6	0.44	NR	66	6.6	27
4	Co–Fe–P-400	LDH	EtOH	6	0.60	NR	78	14	27
5	$NiCo_2O_4$	—	ACN/TBHP	12	2.2	10.4	100	60	121

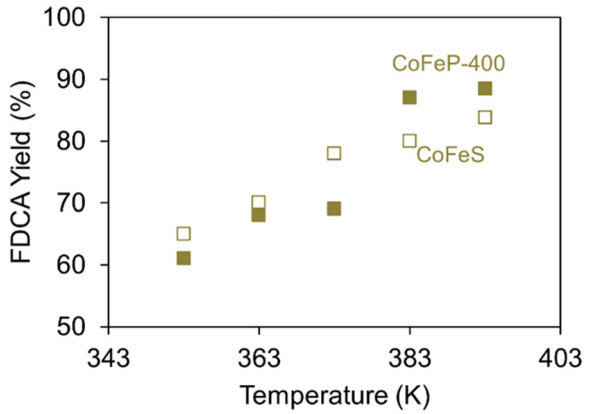

Fig. 23 Temperature effect on FDCA yield of doped Co–Fe catalysts on a layered double hydroxide hydrotalcite support. Reaction conditions: 1 : 1 HMF : catalyst by weight, ACN solvent, 0.61 wt% initial HMF, P = atm, t = 6 h.[27]

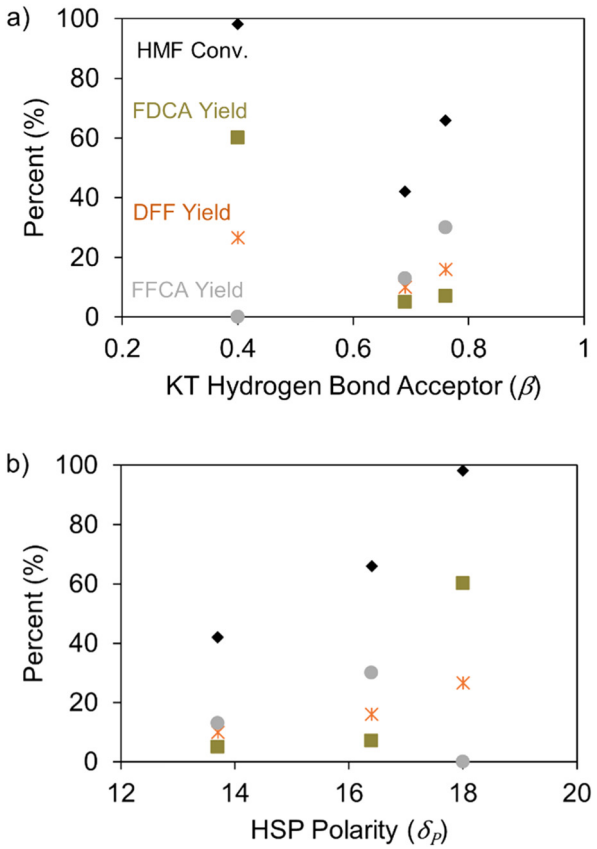

Fig. 24 Effect of solvent (a) hydrogen bond acceptance capacity and (b) polarity on HMF conversion (♦) and FDCA (■), DFF (✳), and FFCA (●) yields for ACN, DMF, and DMSO solvents. Reaction conditions: CoFeP-400/LDH catalyst, 0.36 mL TBHP oxidant additive, 0.44–0.61 wt% HMF, T = 353 K, P_{O_2} = 1 MPa, t = 6 h.[27]

while EtOH (β = 0.75) achieved 78%. Conversion and yields trended more consistently with increasing polarity (Table 8, δ_P), however. ACN, the most polar solvent studied (δ_P = 18.0), had the highest FDCA yields while EtOH (δ_P = 8.8), the least polar, favored primary intermediates like HMFCA and DFF (Fig. 24b).[27]

Yu *et al.*[109] conducted a similar study into a solvent's impact on HMF conversion and product yields. In pure organic solvent systems, all reactions were limited to low FDCA yields (0–6%) with primary selectivity to DFF (Fig. 25a and b) even in alcohol-based solvents (Fig. 25c and d). Considering all solvents, as the β-value increased, both the HMF conversion and DFF yield increased (Fig. 25a and c), which was the opposite trend seen with δ_P (Fig. 25b and d). No significant trends were observed between solvent characteristics and FDCA yields, though insufficient water and O_2 pressure, or the lack of an added oxidant to provide a source of oxygen may have dominated any solvent effects. When the same reaction conditions were applied to a system with more available oxygen, water containing 0.0235 M Na_2CO_3 base additive, HMF conversion improved to 95% and FDCA yield to 88.3%.[109] Increased oxygen availability was also noted as important by Qian *et al.*,[121] who studied the impact of TBHP dosage on FDCA yields in ACN, and by Pandey *et al.*[124] who studied a bimetallic Mn_1Fe_1 catalyst in 46/54 w/w GVL/H_2O both with and without the pretreatment of HMF with ozone. Additionally, adding an ozone pretreatment improved FDCA yields from 40% to 60%, with all other conditions held constant.[124]

Qian *et al.*[121] also found that the catalyst with the largest number of surface defects, and thus the largest amount of adsorbed oxygen in these defects, resulted in the highest yield of FDCA. In their specific study, the 'flaky' morphology of a $NiCo_2O_4$ catalyst contained the highest percentage of adsorbed surface oxygen out of the catalyst variations investigated. This higher oxygen concentration corresponded to the highest observed FDCA yield, 60.1% (Table 11, index 5).[121]

The presence and quantity of acidic/basic sites at the surface of a catalyst remains an important factor in HMF conversion even in organic solvents. For the catalysts reviewed, the presence of graphitic nitrogen and the use of an optimal carbonization temperature for AC supports correlated with increased FDCA yields. When using metal oxide supports, the selection of the correct metal oxide, particularly Al_2O_3, seemed to have the largest impact on such acidic/basic sites. Choosing compatible

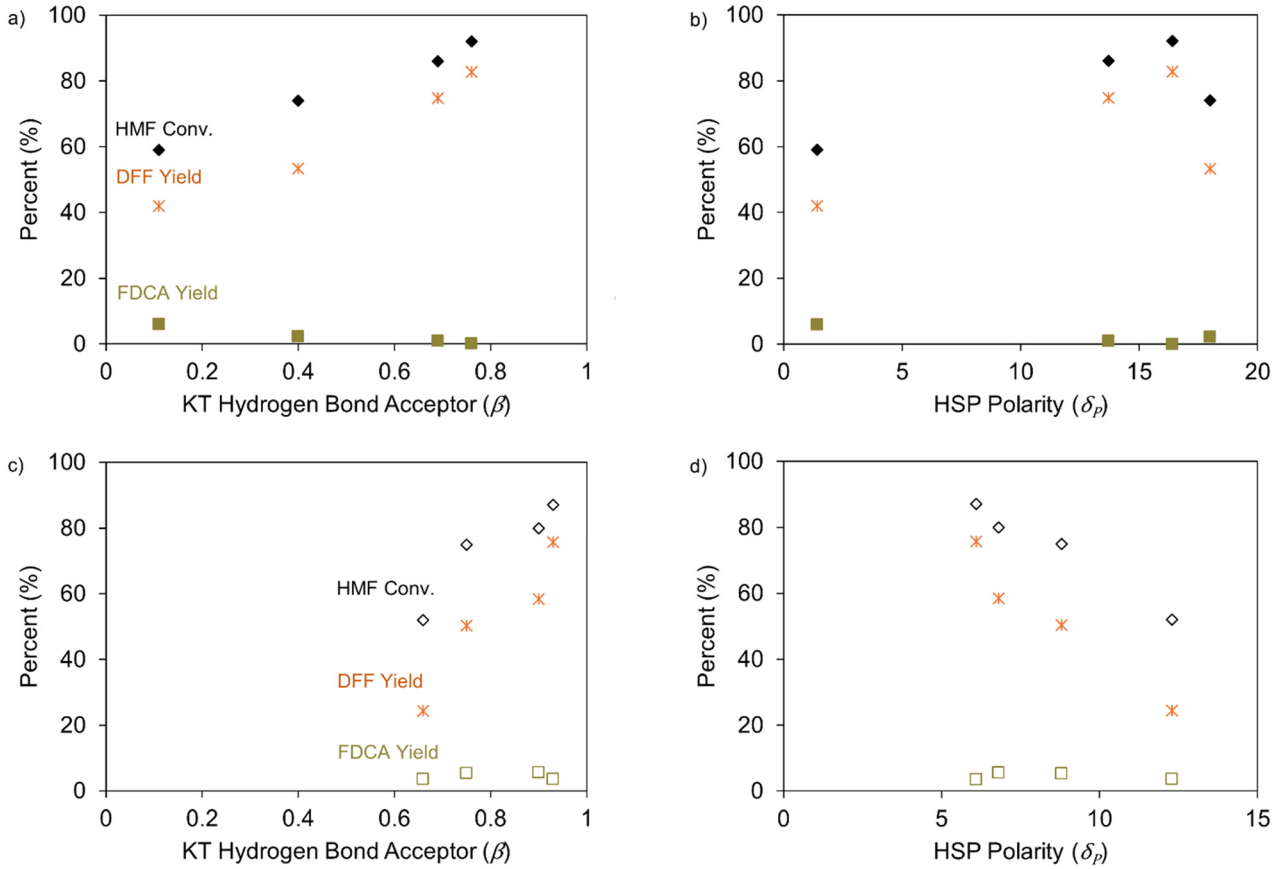

Fig. 25 Trends of HMF conversion (♦), DFF (✳), and FDCA (■) yields for toluene, ACN, DMF, and DMSO pure solvents compared to (a) the KT β parameter and (b) the HSP polarity parameter and the same trends for MeOH, EtOH, *n*-PrOH, and i-PrOH in figure (c) and (d), respectively. Reaction conditions: Co/MnO_2 catalyst, 0.57–0.80 wt% HMF, T = 413 K, P_{O_2} = 0.3 MPa, t = 4 h.[109]

metals for bimetallic catalysts and implementing them in optimal ratios is also important to effectively oxide HMF over NNM catalysts. Additionally, similar to observations with NM catalysts and organics in general, the choice of solvent can significantly impact product selectivity, with solvents prone to accepting hydrogen bonds being more likely to interact with furan functional groups, leading to decreased reactant adsorption at the catalyst surface and hindered reaction progress. Finally, ensuring sufficient oxygen to support the formation of intermediate products and, ultimately, FDCA may be a limiting factor in organic reactions, outweighing the influence of solvent effects.

Conclusions and future outlook

Sustainable and economical production of FDCA remains a critical challenge in the development of bio-derived materials like PEF. To address this, novel solvents, catalysts, and catalyst supports have been investigated in systems both with and without base additives. Recent TEA and LCA studies[9,18,125,126] highlight HMF production as the more critical step compared to FDCA synthesis. This is largely because FDCA yields near 100% can be achieved with various catalysts and reaction conditions, while HMF yields are just 60–90% when using fructose ($600–800 per MT) and 30–60% when using glucose or cellulose ($100–400 per MT). Based on this, future improvements to the commercialization of FDCA should also focus on production of HMF, not only the oxidation of HMF to FDCA. Developing catalysts that may be less active but more tolerant to biomass-derived impurities and using similar solvents for the production of both FDCA and HMF may improve the economics of the process. The use of similar or the same solvents for both processes would eliminate or reduce HMF purification and/or recovery requirements and save the energy required for solvent recovery.

From a catalytic perspective, water remains the preferred solvent due to its low cost, availability, minimal solvent–furan interactions, and the ability to donate oxygen to the reaction. Organic solvents can improve FDCA solubility or allow for the two-step upgrading of sugars directly to FDCA, removing costly purification steps. However, without the presence of water, obtaining FDCA yields close to 100% is more challenging and is unfeasible in many pure-organic systems. Aqueous/organic solvent mixtures seem to be the most promising option for future research. These systems offer the unique advantage of

higher FDCA solubility, which reduces catalyst fouling due to FDCA crystallization, while retaining sufficient water to facilitate high selectivity towards FDCA. Solvent mixtures containing organics with low KT hydrogen bond acceptance basicity (β) and low to moderate polarity (δ_P) tend to correlate with the highest yields of FDCA likely due to minimal interference with furan adsorption to catalyst surfaces.

From a sustainability perspective, organic solvents offer economic and environmental advantages by enabling higher HMF concentrations that decrease energy expenditure considerably; however, solvent stability at reaction conditions, solvent recovery strategies, and catalyst selection need to be carefully studied in the future. A poor organic solvent management strategy may result in higher energy demand compared to aqueous systems, but in either case purification and recovery must be accounted for in LCA and come at a significant cost. Finally, solvent toxicity must also be considered, and in this sense, articles are starting to appear to guide solvent selection. For example, Al Ghatta *et al.*[9] evaluated solvents and concluded that DMSO and ionic liquids would be considered safer than solvents such as methyl isobutyl ketone (MIBK). Other studies, however, indicate that MIBK would be advised before DMSO.[127] Lack of consensus is in part due to differing criteria for the definition of a'safe' or 'sustainable' solvent. Therefore, establishing clear criteria for evaluation is necessary in order to compare different systems and make conclusions concerning scale-up.

Noble metal catalysts such as Pt, Pd, Au, and Ru continue to play a significant role in HMF oxidation, particularly when paired with transition metal oxide or nitrogen-doped carbon supports. Such pairings often result in high conversion of HMF with high selectivity to FDCA. Catalyst characteristics such as high surface area, low metal particle size, even particle distribution, and high concentration of Lewis acidic and basic sites correlate strongly with improved yields. Within the last few years, non-noble metal catalysts such as Ni, Cu, V, Co, Fe, Bi, and Mn, have seen a significant increase in study due to the low cost and lower environmental impact compared to noble metals. These non-noble metal catalysts show high conversion and selectivity towards FDCA, particularly when used as bimetallic catalysts. Specifically, the combined use of metals with different physical properties and valence states has been found to enhance catalytic performance by facilitating better electron transfer and improving reactant adsorption to active sites.

Though non-noble metal catalysts often require longer reaction times or higher temperatures compared to noble metal catalysts, catalyst composition, beneficial doping, and support selection has allowed for competitive performance in some cases. Similarly, though aqueous systems offer the highest FDCA selectivity, they are hindered by low FDCA solubility. Organic solvents improve solubility and allow for higher HMF concentrations but can sometimes interfere with reaction progress through solvent–reactant interactions. The application of aqueous/organic solvent blends, such as GVL/H_2O and DX/H_2O, offer a promising compromise by maintaining selectivity towards FDCA while improving product solubility.

Noble and non-noble metal catalysts are often reported as stable, yet extensive stability studies are rare. Out of 19 studies that included catalyst deactivation performance, only three were done as continuous flow operations, which is necessary to properly evaluate the applicability of a catalyst at commercial scale.[106] The remaining studies were conducted as repeated batch reactions. Even in flow reactor studies, experiments lasted only 40–60 h, which may not have been sufficient time to observe deactivation. Additionally, purified HMF and/or low concentrations of HMF were used as the feedstock, eliminating the effects of impurities on catalyst activity and stability. Extended stability studies at high HMF concentrations and in the presence of biomass-derived impurities should be performed to properly evaluate catalysts for commercial use.

The development of these studies may have a significant effect on TEAs and LCAs. Currently, catalyst selection seems to have a relatively minor effect on both, with catalysts assumed to be stable for years with just minor need for replacement (*i.e.* 10% catalyst make-up).[128] Kim *et al.*[18] reported an increase of 7.9% on the minimum selling price when catalyst stability was reduced from 6 to 3 months (2000 h). In this sense, noble metal catalysts will likely always more stable than non-metals and future research should consider focusing on reducing necessary metal loading on catalysts *via* new synthesis techniques that allow for better utilization of noble metals, or by using bimetallic catalysts that find synergies between noble and non-noble metal catalysts.

Reaction conditions, including temperature, pH, and reaction time, must be optimized to maximize FDCA yield while minimizing HMF degradation. The synergistic interplay of solvent, catalyst, support, additives, and reaction conditions ultimately dictate the efficiency of HMF conversion and selectivity towards FDCA. Continued research into non-noble metal catalysts and aqueous/organic solvent mixtures for HMF upgrading presents ongoing opportunities to enhance FDCA yields and ultimately achieve the economic viability of FDCA production.

Future research on HMF oxidation to produce FDCA will likely focus on improving catalyst activity and reusability, particularly for non-noble metal systems, optimizing solvent selection to minimize adverse solvent–reactant interactions, and the expanding application of alternate oxidative techniques like electrocatalysis and photocatalysis. This research will have to be integrated with TEAs and LCAs where the oxidation of HMF is studied alongside its production.

Author contributions

J. M. M.: conceptualization, data curation, analysis, undergraduate supervision, visualization, writing – original manuscript preparation, revision, and formatting. J. S.: conceptualization, data curation, analysis, undergraduate supervision, visualization, writing – original manuscript preparation, revision, and formatting. V. L.: data curation, visualization, writing – review and editing. Z. F.: data curation, writing – reviewing and editing. D. M. A.: data curation, analysis, writing – reviewing and editing.

S. G. W.: conceptualization, analysis, funding acquisition, supervision, visualization, writing – original manuscript preparation, revision, and formatting. All authors have given approval to the final version of the manuscript.

Data availability

No primary research results, software or code have been included and no new data were generated or analyzed as part of this review. All data is available in existing literature as referenced in the review paper.

Conflicts of interest

The authors declare no conflicts of interest.

Acknowledgements

The authors are grateful for the support of the National Science Foundation CBET, grant no. 2230355. Any opinions, findings, conclusions, or recommendations expressed in this material are those of the author(s) and do not necessarily reflect the views of the National Science Foundation. Additionally, Van Ledger would like to thank the MSU Undergraduate Scholars Program and Zach Fredericks would like to thank the Montana Space Grant Consortium Awards for Research in Engineering and Science (ARES) for funding. During the preparation of this work, the authors used ChatGPT in order to improve the readability and concision of the document. After using this tool/service, the authors reviewed and edited the content as needed and took full responsibility for the content of the publication.

References

1 T. A. Werpy and G. Petersen, NREL/TP-510-35523, National Renewable Energy Lab., Golden, CO (US), 2004.
2 J. J. Bozell and G. R. Petersen, *Green Chem.*, 2010, **12**, 539–554.
3 E. de Jong, H. A. Visser, A. S. Dias, C. Harvey and G.-J. M. Gruter, *Polymers*, 2022, **14**, 943.
4 J. Stanley, Z. Terzopoulou, P. A. Klonos, A. Zamboulis, E. Xanthopoulou, S. Koltsakidis, D. Tzetzis, L. F. Zemljič, D. A. Lambropoulou, A. Kyritsis, G. Z. Papageorgiou and D. N. Bikiaris, *Polymers*, 2023, **15**, 2707.
5 E. Forestier, C. Combeaud, N. Guigo and N. Sbirrazzuoli, *Polymers*, 2023, **15**, 661–678.
6 M. Plum, *et al.* Case Studies Based on Peer-reviewed Life Cycle Assessments – Carbon Footprints on Different Renewable Carbon-based Chemicals and Materials, **https://renewable-carbon.eu/publications/product/rci-scientific-background-report-2023/**, (accessed October 13, 2024).
7 P. Lokhande, K. Sonone and P. L. Dhepe, *New J. Chem.*, 2023, **47**, 15325–15335.
8 P. Stegmann, T. Gerritse, L. Shen, M. Londo, Á. Puente and M. Junginger, *J. Cleaner Prod.*, 2023, **395**, 136426.
9 A. Al Ghatta, J. D. E. T. Wilton-Ely and J. P. Hallett, *Green Chem.*, 2021, **23**, 1716–1733.
10 J. Cai, K. Li and S. Wu, *Biomass Bioenergy*, 2022, **158**, 106358.
11 C. Chen, L. Wang, B. Zhu, Z. Zhou, S. I. El-Hout, J. Yang and J. Zhang, *J. Energy Chem.*, 2021, **54**, 528–554.
12 Y. Lu, C. Lin, H. Yang, P. Ma, J. Chen, Z. He, H. Wu, F. Cao, K. Chen and P. Ouyang, *Biomass Convers. Biorefin.*, 2024, **14**, 20105–20115.
13 X. Zuo, P. Venkitasubramanian, D. H. Busch and B. Subramaniam, *ACS Sustainable Chem. Eng.*, 2016, **4**, 3659–3668.
14 A. Jasi, Avantium commercialising PEF production. The Chemical Engineer, 2018, May 31, **https://www.thechemicalengineer.com/news/avantium-commercialising-pef-production/** (accessed January 2025).
15 J. Louw, S. Farzad and J. F. Görgens, *Biofuels, Bioprod. Biorefin.*, 2023, **17**, 135–152.
16 C. Chen, M. Lv, H. Hu, L. Huai, B. Zhu, S. Fan, Q. Wang and J. Zhang, *Adv. Mater.*, 2024, **36**, 2311464.
17 M. G. Davidson, S. Elgie, S. Parsons and T. J. Young, *Green Chem.*, 2021, **23**, 3154–3171.
18 H. Kim, S. Baek and W. Won, *Renewable Sustainable Energy Rev.*, 2022, **157**, 112059.
19 S. Li, S. Wang, Y. Wang, J. He, K. Li, Y. Xu, M. Wang, S. Zhao, X. Li and X. Zhong, *Adv. Funct. Mater.*, 2023, **33**, 2214488.
20 Y. Peng, B. Qiu, S. Ding, M. Hu, Y. Zhang, Y. Jiao, X. Fan and C. M. Parlett, *ChemPlusChem*, 2024, **89**, e202300545.
21 K. Wadaugsorn, K.-Y. Lin, A. Kaewchada and A. Jaree, *RSC Adv.*, 2022, **12**, 18084–18092.
22 Y. Wei, C. Li, C. Zhu, Y. Zhang, Z. Zhu, Y. Chen, X. Li and Y. Yan, *J. Taiwan Inst. Chem. Eng.*, 2022, **138**, 104439.
23 K. T. V. Rao, Y. Hu, Z. Yuan, Y. Zhang and C. C. Xu, *Chem. Eng. J.*, 2021, **404**, 127063.
24 W. Guan, Y. Zhang, Y. Chen, J. Wu, Y. Cao, Y. Wei and P. Huo, *J. Catal.*, 2021, **396**, 40–53.
25 M. Mani, M. Mariyaselvakumar, S. Tothadi, A. B. Panda, K. Srinivasan and L. J. Konwar, *Mol. Catal.*, 2024, **554**, 113811.
26 A. E. Demet, O. Gimello, R. Arletti, N. Tanchoux, M. T. Sougrati, L. Stievano, F. Quignard, G. Centi, S. Perathoner and F. Di Renzo, *Catalysts*, 2022, **12**, 814–839.
27 D. Gao, F. Fang, G. I. Waterhouse, F. Han and Y. Li, *Catal. Sci. Technol.*, 2024, **14**, 1191–1200.
28 S. Hameed, W. Liu, Z. Yu, J. Pang, W. Luo and A. Wang, *Green Chem.*, 2024, **26**, 7806–7817.
29 G. Lin, W. Lin, J. Wu, Y. Zhan, F. Okejiri, M. Weng and J. Fu, *Chem. Eng. Sci.*, 2022, **249**, 117343.
30 S. Somsri, A. Prasertsab, P. Pornsetmetakul, N. Maineawklang, M. T. Nguyen, T. Yonezawa and C. Wattanakit, *Microporous Mesoporous Mater.*, 2023, **354**, 112559.
31 Clarivate, Web of Science, (accessed January 25, 2025).
32 Y. Jin, S. Sarina, H. Liu, W. Martens, E. R. Waclawik, E. Peiris, J. Jia, J. Shang, L. Kou and C. Guo, *ACS Catal.*, 2022, **12**, 11226–11238.

33 N. Thiensuwan, S. Sankaranarayanan, T. Yokoi and C. Ngamcharussrivichai, *ACS Sustainable Chem. Eng.*, 2023, **11**, 11424–11436.
34 J. M. Molinaro, M. R. Carroll, A. S. Young and S. G. Wettstein, *ACS Omega*, 2024, **9**, 30708–30716.
35 H. Ban, T. Pan, Y. Cheng, L. Wang and X. Li, *J. Chem. Eng. Data*, 2018, **63**, 1987–1993.
36 A. H. Motagamwala, W. Y. Won, C. Sener, D. M. Alonso, C. T. Maravelias and J. A. Dumesic, *Sci. Adv.*, 2018, **4**, eaap9722.
37 J. Kim, J.-C. Kim, Y.-M. Cho, C.-H. Yoon, H. W. Kwak, J.-H. Choi, H. Kim and I.-G. Choi, *Biomass Bioenergy*, 2024, **181**, 107049.
38 L. Yu, H. Chen, Z. Wen, X. Ma, Y. Li and Y. Li, *Ind. Eng. Chem. Res.*, 2021, **60**, 13485–13491.
39 Z. Ma, L. Wang, G. Li and T. Song, *Catalysts*, 2024, **14**, 157.
40 F. Pardo Pardo, H. Oorts, A. M. Urtiaga Mendia, J. Esteban Serrano and G. Zarca Lago, *J. Mol. Liq.*, 2024, **409**, 125436.
41 G. Nawaz, M. Fatima, Z. Ahmad, K. S. Joya, M. A. Assiri, S. I. A. Shah, F. Yasmeen and M. N. Khan, *Fuel*, 2024, **362**, 130828.
42 W. Wang, H. Xu, T. Sang, D. Ji, J. Hao and Z. Li, *Chem. Commun.*, 2024, **60**, 4214–4217.
43 T. Wei, W. Liu, S. Zhang, Q. Liu, J. Luo and X. Liu, *Chem. Commun.*, 2023, **59**, 442–445.
44 Z. Lin, L. Wang, T. Jia, X. Wang, C. Li, H. Wang, L. Li, Y. Zhou, C. Zhai and H. Tao, *Chem. Eng. J.*, 2024, **481**, 148429.
45 Y. Wang, H. Chen, Y. Tang and Y. Li, *Int. J. Hydrogen Energy*, 2024, 162–183.
46 Y. Lin, H. Wang, Y. Zhou and Y. Wu, *J. Mol. Struct.*, 2025, **1322**, 140404.
47 M. Umair, C. M. Pecoraro, F. Di Franco, M. Santamaria, L. Palmisano, V. Loddo and M. Bellardita, *Sustainable Mater. Technol.*, 2025, **43**, e01188.
48 S. Prasad, A. J. Khalid, V. Narishetty, V. Kumar, S. Dutta and E. Ahmad, *Mater. Sci. Energy Technol.*, 2023, **6**, 501–521.
49 S. Chen, X. Guo, H. Ban, T. Pan, L. Zheng, Y. Cheng, L. Wang and X. Li, *Ind. Eng. Chem. Res.*, 2021, **60**, 16887–16898.
50 L. Yang, J. Liu, F. Cheng, S. Zhou, Q. Xu, D. Yin and X. Liu, *Renewable Energy*, 2024, **226**, 120409.
51 S. Das, G. Cibin and R. I. Walton, *ACS Sustainable Chem. Eng.*, 2024, **12**, 5575–5585.
52 G. Y. Ryu, D. Park, Y. Jo, C. C. Truong, D. K. Mishra and Y.-W. Suh, *Biomass Bioenergy*, 2024, **180**, 107022.
53 B. S. Rao, M. J. Hidajat, G.-N. Yun and D. W. Hwang, *Catal. Sci. Technol.*, 2023, **13**, 6921–6936.
54 G. Chen, L. Zheng, Q. Sun and B. Zong, *Mol. Catal.*, 2024, **552**, 113677.
55 J. Xie, J. Nie and H. Liu, *Chin. J. Catal.*, 2014, **35**, 937–944.
56 S. E. Davis, A. D. Benavidez, R. W. Gosselink, J. H. Bitter, K. P. De Jong, A. K. Datye and R. J. Davis, *J. Mol. Catal. A: Chem.*, 2014, **388**, 123–132.
57 Z. Li, E. Du, P. Hao, L. Huai, Y. Zhong, S. I. El-Hout, C. Chen and J. Zhang, *Catal. Today*, 2023, **423**, 114277.
58 Q. Hou, T. Gao, H. Zhang, Q. Tang and W. Fang, *Catal. Today*, 2025, **443**, 114990.
59 J. O. P. Broekman and P. J. Deuss, *Organometallics*, 2024, **43**, 1264–1275.
60 M.-K. Ke, Y. Min, S.-C. Mei, H.-W. Zeng, Z.-H. Wang, T.-W. Hua, J.-J. Chen, G.-X. Huang and H.-Q. Yu, *Appl. Catal., B*, 2024, **358**, 124431.
61 S. Kar, Q.-Q. Zhou, Y. Ben-David and D. Milstein, *J. Am. Chem. Soc.*, 2022, **144**, 1288–1295.
62 D. Zhao, T. Su, Y. Wang, R. S. Varma and C. Len, *Mol. Catal.*, 2020, **495**, 111133.
63 A. Laurell Nash, R. Hertzberg, Y. Q. Wen, B. Dahlgren, T. Brinck and C. Moberg, *Chem. – Eur. J.*, 2016, **22**, 3821–3829.
64 Z. Zhang, B. Liu, K. Lv, J. Sun and K. Deng, *Green Chem.*, 2014, **16**, 2762–2770.
65 D. Zeng, W. Wang, B. Cui, B. Jiang, C. Zhang, L. Zhang and W. Wang, *Fuel*, 2025, **381**, 133238.
66 S. Zhang, G. Chu, S. Wang, J. Ma and C. Wang, *Molecules*, 2024, **29**, 3213.
67 B. Chen, Y. Abe, H. Guo and R. L. Smith Jr, *Fuel*, 2024, **376**, 132745.
68 E. J. de Boed, H. L. Nolten, N. Masoud, R. Vogel, F. Wang, Z. Xu, E. J. Doskocil, B. Donoeva and P. E. de Jongh, *ChemCatChem*, 2024, **16**, e202301436.
69 H. B. Rose, T. Greinert, C. Held, G. Sadowski and A. S. Bommarius, *J. Chem. Eng. Data*, 2018, **63**, 1460–1470.
70 K. R. Vuyyuru and P. Strasser, *Catal. Today*, 2012, **195**, 144–154.
71 S. E. Davis, L. R. Houk, E. C. Tamargo, A. K. Datye and R. J. Davis, *Catal. Today*, 2011, **160**, 55–60.
72 H. Moradi, S. A. Kulinich, W. Wunderlich and M. Ghiaci, *ChemistrySelect*, 2024, **9**, e202303246.
73 J. Su, Z. Liu, Y. Tan, Y. Xiao, N. Zhan and Y. Ding, *Molecules*, 2024, **29**, 2724.
74 T. Seehamongkol, B. Rungtaweevoranit, P. Chakthranont, T. Butburee, W. Nimsaila and K. Faungnawakij, *ChemNanoMat*, 2024, **10**, e202400037.
75 S. Zhang, Y. Yang, G. Chu, S. Wang, C. Wang, Y. Zhang, L. Zhang and J. Mei, *Chem. Eng. J.*, 2023, **474**, 145670.
76 V. Parmon, V. Simagina and L. Milova, *Catal. Ind.*, 2010, **2**, 199–205.
77 J. D. Hayler, D. K. Leahy and E. M. Simmons, *Organometallics*, 2018, **38**, 36–46.
78 S. E. Davis, B. N. Zope and R. J. Davis, *Green Chem.*, 2012, **14**, 143–147.
79 C. Yang, X. Li, Z. Zhang, B. Lv, J. Li, Z. Liu, W. Zhu, F. Tao, G. Lv and Y. Yang, *Fuel*, 2020, **278**, 118361.
80 C. Chen, X. Li, L. Wang, T. Liang, L. Wang, Y. Zhang and J. Zhang, *ACS Sustainable Chem. Eng.*, 2017, **5**, 11300–11306.
81 Y. Zhao, J. Baeza, N. K. Rao, L. Calvo, M. Gilarranz, Y. Li and L. Lefferts, *J. Catal.*, 2014, **318**, 162–169.
82 K. D. Baugh and P. L. McCarty, *Biotechnol. Bioeng.*, 1988, **31**, 50–61.
83 T. S. Kharlamova, K. L. Timofeev, D. P. Morilov, M. A. Salaev, A. I. Stadnichenko, O. A. Stonkus and O. V. Vodyankina, *React. Chem. Eng.*, 2024, **9**, 2691–2709.

84 S. Xie, H. Tsunoyama, W. Kurashige, Y. Negishi and T. Tsukuda, *ACS Catal.*, 2012, **2**, 1519–1523.
85 R. Zanella and C. Louis, *Catal. Today*, 2005, **107**, 768–777.
86 S. K. Perumal, S. Lee, H. Yu, J. Heo, M. J. Kang, Y. Kim, M. Park, H. Lee and H. S. Kim, *ACS Appl. Mater. Interfaces*, 2024, **16**, 7353–7363.
87 L. Zheng, J. Zhao, Z. Du, B. Zong and H. Liu, *Sci. China: Chem.*, 2017, **60**, 950–957.
88 J. Zhang, P. Chen, H. Liu, R. Zhang, W. Jia, J. Zhang and L. Peng, *Appl. Catal., A*, 2024, **676**, 119663.
89 R. Mu, Z.-J. Zhao, Z. Dohnálek and J. Gong, *Chem. Soc. Rev.*, 2017, **46**, 1785–1806.
90 A. Ruiz Puigdollers, P. Schlexer, S. Tosoni and G. Pacchioni, *ACS Catal.*, 2017, **7**, 6493–6513.
91 H. Metiu, S. Chrétien, Z. Hu, B. Li and X. Sun, *J. Phys. Chem. C*, 2012, **116**, 10439–10450.
92 I. Herlina, Y. K. Krisnandi and M. Ridwan, *S. Afr. J. Chem. Eng.*, 2024, **47**, 75–82.
93 D. Gao, F. Han, G. I. Waterhouse, Y. Li and L. Zhang, *Biomass Convers. Biorefin.*, 2024, **14**, 13707–13719.
94 Y. Gao, S. Fan, B. Zhu, S. I. El-Hout, J. Lyu, J. Zhang and C. Chen, *Catal. Today*, 2024, **440**, 114847.
95 M. Rao, M. Wang, X. Zheng, D. Pan, C. Hong, K. Chen and L. Lin, *Chem. Eng. Sci.*, 2022, **262**, 118004.
96 M. Zhang, P. Che, H. Ma, X. Liu, S. Zhang, Y. Luo and J. Xu, *Chin. J. Catal.*, 2024, **67**, 144–156.
97 Q. Zhang, A. Chen, W. Pan and H. Zhu, *New J. Chem.*, 2024, **48**, 4054–4062.
98 Z. Wang, S. Xia, X. Wang, Y. Fan, K. Zhao, S. Wang, Z. Zhao and A. Zheng, *Renewable Sustainable Energy Rev.*, 2024, **196**, 114332.
99 H. S. Le, Z. Said, M. T. Pham, T. H. Le, I. Veza, B. Deepanraj and L. H. Nguyen, *Fuel*, 2022, **324**, 124474.
100 Y. Wang, C. A. Brown and R. Chen, *AIMS Microbiol.*, 2018, **4**, 261.
101 M. J. Antal Jr, W. S. Mok and G. N. Richards, *Carbohydr. Res.*, 1990, **199**, 91–109.
102 J. E. Romo, N. V. Bollar, C. J. Zimmermann and S. G. Wettstein, *ChemCatChem*, 2018, **10**, 4805–4816.
103 S. G. Wettstein, D. M. Alonso, E. I. Gürbüz and J. A. Dumesic, *Curr. Opin. Chem. Eng.*, 2012, **1**, 218–224.
104 Y. Román-Leshkov, J. N. Chheda and J. A. Dumesic, *Science*, 2006, **312**, 1933–1937.
105 Y. Román-Leshkov and J. A. Dumesic, *Top. Catal.*, 2009, **52**, 297–303.
106 J. Iglesias, I. Martínez-Salazar, P. Maireles-Torres, D. M. Alonso, D. R. Mariscal and M. L. Granados, *Chem. Soc. Rev.*, 2020, **49**, 5704–5771.
107 Y. Z. Zhang, X. Guo, P. Tang and J. Xu, *J. Chem. Eng. Data*, 2018, **63**, 1316–1324.
108 N. H. Zhuang, J. C. Wang, S. Ma, Q. Liu, W. L. Jia, X. Yu, Z. Li, S. L. Yang, Y. Sun, X. Tang, X. H. Zeng and L. Lin, *J. Chem. Eng. Data*, 2023, **68**, 726–743.
109 L. Yu, J. Mao, Y. Chen, G. Zhang and X. Chen, *Catal. Lett.*, 2024, **154**, 5555–5560.
110 B. Tharat, L. Ngamwongwan, T. Seehamongkol, B. Rungtaweevoranit, J. Nonkumwong, S. Suthirakun, K. Faungnawakij, N. Chanlek, A. Plucksacholatarn and W. Nimsaila, *Nanoscale*, 2024, **16**, 678–690.
111 C. M. Hansen, *Hansen Solubility Parameters: A User's Handbook*, CRC Press, Boca Raton, FL, 2 edn, 2007.
112 M. J. Kamlet, J. L. M. Abboud, M. H. Abraham and R. Taft, *J. Org. Chem.*, 1983, **48**, 2877–2887.
113 J. Liu, F. Cheng, S. Zhou, L. Zhu, Q. Xu, D. Yin and X. Liu, *Mol. Catal.*, 2024, **560**, 114141.
114 L. Xu, J. Fu, C. Du, Q. Xu, B. Liu and Z. Bao, *Processes*, 2022, **10**, 2480.
115 R. Stenutz, Kamlet-Taft solvent parameters, **https://www.stenutz.eu/chem/kamlettaft.php?s=1&p=0**, 2024).
116 S. Abbott and H. Yamamoto, *HSPiP Software*, 2020.
117 C. F. Brayton, *Cornell Vet.*, 1986, **76**, 61–90.
118 P. Góralski, *J. Chem. Soc., Faraday Trans. 1*, 1988, **84**, 4311–4316.
119 N. A. Abduh, A. Al-Kahtani, T. S. Algarni and A.-B. Al-Odayni, *Catalysts*, 2023, **13**, 692.
120 C. Y. Y. Wong, A. W.-T. Choi, M. Y. Lui, B. Fridrich, A. K. Horváth, L. T. Mika and I. T. Horváth, *Struct. Chem.*, 2017, **28**, 423–429.
121 H. Qian, Y. He, Q. Hou, C. Xie, R. Lai, G. Yu, T. Xia, X. Bai, H. Xie and M. Ju, *Green Energy Environ.*, 2024, DOI: **10.1016/j.gee.2024.05.002**.
122 B. Liu, S. Xu, M. Zhang, X. Li, D. Decarolis, Y. Liu, Y. Wang, E. K. Gibson, C. R. A. Catlow and K. Yan, *Green Chem.*, 2021, **23**, 4034–4043.
123 M. Zhang, Y. Liu, B. Liu, Z. Chen, H. Xu and K. Yan, *ACS Catal.*, 2020, **10**, 5179–5189.
124 S. Pandey, M. Mottoul, V. Orsat, J.-F. Morin and M.-J. Dumont, *J. Environ. Chem. Eng.*, 2024, **12**, 112763.
125 S. Bello, P. Méndez-Trelles, E. Rodil, G. Feijoo and M. T. Moreira, *Sep. Purif. Technol.*, 2020, **233**, 116056.
126 P. Patel, D. Schwartz, X. Wang, R. Lin, O. Ajao and A. Seifitokaldani, *ACS Sustainable Chem. Eng.*, 2022, **10**, 4206–4217.
127 D. Prat, A. Wells, J. Hayler, H. Sneddon, C. R. McElroy, S. Abou-Shehada and P. J. Dunn, *Green Chem.*, 2016, **18**, 288–296.
128 S. M. Sen, D. M. Alonso, S. G. Wettstein, E. I. Gürbüz, C. A. Henao, J. A. Dumesic and C. T. Maravelias, *Energy Environ. Sci.*, 2012, **5**, 9690–9697.